haematologica
Journal of the Ferrata Storti Foundation

Pharmacological blockade of rho kinase enhances venetoclax responses in translational models of acute myeloid leukemia

by Upendarrao Golla, Riya Bhalodia, Charyguly Annageldiyev, Satyam Patel, Vishnu Sravan Bollu, Su-Fern Tan, Myles C. Cabot, David J. Feith, Thomas P. Loughran, Ross L. Levine, Shin Mineishi, Hong Zheng, Kentaro Minagawa, Jeremy Hengst, Giselle L. Saulnier Sholler, Dhimant Desai, Sinisa Dovat, Kelsey H. Fisher-Wellman, David F. Claxton and Arati Sharma

Received: August 25, 2025.
Accepted: March 25, 2026.

Citation: Upendarrao Golla, Riya Bhalodia, Charyguly Annageldiyev, Satyam Patel, Vishnu Sravan Bollu, Su-Fern Tan, Myles C. Cabot, David J. Feith, Thomas P. Loughran, Ross L. Levine, Shin Mineishi, Hong Zheng, Kentaro Minagawa, Jeremy Hengst, Giselle L. Saulnier Sholler, Dhimant Desai, Sinisa Dovat, Kelsey H. Fisher-Wellman, David F. Claxton and Arati Sharma.

Haematologica. 2026 Apr 2. doi: 10.3324/haematol.2025.289041 [Epub ahead of print]

Title: Pharmacological blockade of rho kinase enhances venetoclax responses in translational models of acute myeloid leukemia

Running Title: Targeting ROCK improves venetoclax response in AML

Author List and Affiliations:
Upendarrao Golla[1], Riya Bhalodia[2,†], Charyguly Annageldiyev[1], Satyam Patel[2], Vishnu Sravan Bollu[1,2], Su-Fern Tan[3,4], Myles C. Cabot[4], David J. Feith[3,4], Thomas P. Loughran Jr.[3,4], Ross L. Levine[5,6], Shin Mineishi[1], Hong Zheng[1], Kentaro Minagawa[1], Jeremy Hengst[7], Giselle L. Saulnier Sholler[7], Dhimant Desai[2,8], Sinisa Dovat[7], Kelsey H. Fisher-Wellman[9], David F. Claxton[1,8], Arati Sharma[2,8,#]

[1]Division of Hematology and Oncology, Department of Medicine, Pennsylvania State University College of Medicine, Hershey, PA, USA
[2]Department of Molecular and Precision Medicine, Pennsylvania State University College of Medicine, Hershey, PA, USA
[3]Department of Medicine, Division of Hematology & Oncology, University of Virginia School of Medicine, Charlottesville, VA, USA
[4]University of Virginia Comprehensive Cancer Center, Charlottesville, VA, USA
[5]Human Oncology and Pathogenesis Program, Memorial Sloan Kettering Cancer Center, New York, NY, USA
[6]Leukemia Service, Department of Medicine and Center for Hematologic Malignancies, Memorial Sloan Kettering Cancer Center, New York, NY, USA
[7]Division of Hematology and Oncology, Department of Pediatrics, Pennsylvania State University, College of Medicine, Hershey, PA, USA
[8]Penn State Cancer Institute, Pennsylvania State University College of Medicine, Hershey, PA, USA
[9]Department of Cancer Biology, Atrium Health Wake Forest Baptist Comprehensive Cancer, Wake Forest University School of Medicine, Winston-Salem, NC, USA
[†]Current address: Saint Louis University School of Medicine, Saint Louis, MO, USA

[#]**Corresponding Author:**
Arati Sharma, Ph.D.
Department of Molecular and Precision Medicine, Pennsylvania State University College of Medicine, Hershey, PA 17033
Phone: 717-531-0003 (ext. 289551); E-mail: asharma@pennstatehealth.psu.edu

Data Availability Statement: The authors confirm that the data supporting the findings of this study are available within the article and/or its online Supplementary Appendix. Additional information is available upon request from the corresponding author.

Author Contributions: UG, AS and DFC conceptualized the study design. UG, RB, CA, SP, VSB, SFT, KFW, and AS were responsible for experimental work, data collection, and data analysis. MCC, DJF, KFW, JH, GLS, DD, RLL, SM, HZ, KM, SD, and TPL provided scientific resources and subject matter expertise. AS and DFC provided project oversight. AS, DFC, and TPL were responsible for the funding acquisition. UG drafted the original manuscript with the inputs from AS and DFC. UG, VSB, and AS revised the manuscript. All co-authors provided edits, reviewed, and approved the final manuscript.

Disclosures: DJF has received research funding, honoraria, and/or stock options from AstraZeneca, Dren Bio, Recludix Pharma, and Kymera Therapeutics. TPL has received Scientific Advisory Board membership, consultancy fees, honoraria, and/or stock options from Keystone Nano, Flagship Labs 86, Dren Bio, Recludix Pharma, Kymera Therapeutics, and Prime Genomics. RLL is a scientific advisor to Imago, Mission Bio, Zentalis, Ajax, Auron, Prelude, C4 Therapeutics, and Isoplexis. He receives research support from Ajax, Zentalis, and Abbvie; has consulted for Incyte, Janssen, and Astra Zeneca; and has received honoraria from Astra Zeneca for invited lectures. Other authors declare no competing interests. The funders had no role in the design of this study; in the collection, analyses, or interpretation of data; in the writing of this manuscript; or in the decision to publish the results.

Acknowledgements: The authors would like to acknowledge and thank the patients and their families who supported our studies. The authors thank those who generously provided cell lines for our studies: Barbara Miller, Penn State Hershey (U937); Xiaorong Gu, Cleveland Clinic (OCI-AML2 and OCI-AML3); and H.G. Wang, Penn State Hershey (MOLM-13, MOLM-13-YFP-Luc). The authors thank Mosammat Begom and Avinash Kudva (Penn State College of Medicine) for technical help. The authors thank the staff of the Department of Comparative Medicine, Bioluminescence Imaging Core (RRID: SCR_023179), Flow Cytometry Core (RRID:SCR_021134), Organic Synthesis Core (RRID:SCR_012425), Four Diamonds Developmental Therapeutic Preclinical Core, and Molecular and Histopathology Core facilities at the Penn State University College of Medicine. The authors thank the Penn State Cancer Institute, the Department of Molecular and Precision Medicine, the Kenneth F. Noel Memorial Fund (AS), the Delbert J. McQuaide Cancer Research Fund (AS), and the Four Diamond Transformative Fund (AS). This work was partly supported by the subaward funds to DFC from the National Institutes of Health (NIH) under the National Cancer Institute (NCI) award number P01 CA171983 (TPL). The content is solely the responsibility of the authors and does not necessarily represent the official views of the NIH or NCI.

Abstract:

Acute Myeloid Leukemia (AML) is an aggressive hematologic malignancy requiring concomitant targeting of critical cellular survival pathways due to resistance and frequent relapse with monotherapies. Venetoclax (VEN), a BCL-2 inhibitor, is one such promising clinical agent best utilized in combination therapies due to transient responses and acquired resistance. Given the involvement of the Rho/ROCK pathway in VEN activity, we combined Rho-associated coiled-coil–containing protein kinase inhibitors (ROCKi))with VEN to achieve superior antileukemic activity. The ROCKi (Fasudil, DJ4, GSK269962A) synergized with VEN to enhance cytotoxicity in both VEN-sensitive and VEN-resistant cell lines *in vitro*. Among the three ROCKi, GSK269962A (GSK) was best-tolerated in combination with VEN and effectively inhibited leukemia growth across multiple AML cell line-derived xenograft models *in vivo*. The GSK+VEN combination exhibited additive to synergistic cytotoxicity in primary AML patient cells *ex vivo* and enhanced antileukemic activity in a patient-derived xenograft model. Additionally, the GSK+VEN combination significantly decreased the clonogenicity of primary AML cells, relatively sparing normal cells. Functional assays demonstrated enhanced apoptosis (Annexin V, caspase-3/7), elevated reactive oxygen species, and mitochondrial depolarization in both VEN-sensitive and VEN-resistant AML cells following combination treatment. Mechanistically, GSK augmented venetoclax responses by downregulating anti-apoptotic proteins (BCL2, MCL1) and inducing pro-apoptotic mediators (NOXA, MCL1 short isoforms), including in VEN-resistant AML cells. Together, these findings across multiple preclinical AML models demonstrate synergistic antileukemic activity and support combining VEN with ROCKi as a promising therapeutic strategy for AML.

Introduction:

Acute myeloid leukemia (AML) remains among the most lethal leukemias, with a 5-year overall survival rate of only 32.9%.[1] Despite significant research efforts, improvements in AML survival outcomes over the past two decades have been relatively modest. Relatively few patients can tolerate intensive chemotherapy or allogeneic stem cell transplantation.[2-4] Though there have been significant advances in lower-intensity therapy options in recent years,[3,4] further efforts are needed to achieve improved remission and survival rates among older adults and patients who are unfit for intensive chemotherapy.

The approval of the anti-apoptotic B-cell lymphoma 2 (BCL-2) inhibitor venetoclax (VEN; also known as ABT-199) in combination with hypomethylating agents or low-dose cytarabine (LDAC) was a significant milestone for AML patients ineligible for intensive chemotherapy, both in the frontline and relapsed or refractory (R/R) settings. While VEN-based regimens achieve response rates of approximately 54-74% in newly diagnosed AML, these rates decline to 20-40% in patients with R/R AML.[3,5-8] VEN combination regimens are not curative, and nearly all patients develop resistance to VEN and are refractory or progress within two years.[7] Therefore, there is a critical unmet need for effective, well-tolerated treatment strategies that can enhance response rates to VEN in AML patients.

To better understand VEN resistance, Chen et al.[9] performed a genome-wide CRISPR/Cas9 loss-of-function screen with VEN in MOLM-13 AML cells and identified several “sensitizer” genes (i.e. associated with improved VEN response), including the Rho/ROCK (Rho-associated protein kinase) pathway. Similarly, ROCK1 was elevated in the secretome of AML patients with high anti-apoptotic index.[10] More recent work has demonstrated that rho-kinases ROCK1/2 are upregulated in AML cells that are resistant to VEN and doxorubicin.[11,12] These findings suggest that rho-kinases play an antiapoptotic role, and inhibition of ROCK activity may synergize with VEN and overcome VEN resistance to effectively induce apoptotic cell death in AML.

The Rho/ROCK signaling pathway regulates actin cytoskeletal dynamics, cell migration, and various cellular processes including cell proliferation, differentiation, survival, and apoptosis.[13,14] ROCK1/2, Ser/Thr protein kinases, have aided in the development and progression of various cancers including AML, and drug

resistance.[11-13,15,16] Over the last decade, ROCK inhibitors (ROCKi) such as fasudil, DJ4, and GSK269962A (GSK) have been explored as potential therapeutic agents for AML.[17-19] However, the use of ROCKi in combination therapy for AML remains largely underexplored.

Here, we evaluated the activity of ROCKi in combination with VEN for the effective treatment of AML and the circumvention of VEN resistance. The combination synergistically induced cytotoxicity in AML cell lines *in vitro* and primary AML patient samples *ex vivo*. The addition of GSK enhanced VEN activity by downregulating survival proteins and promoting the expression of proapoptotic proteins in both naïve and VEN-resistant AML cells. *In vivo* results show that GSK potentiated the efficacy of VEN in multiple cell line-derived xenografts (CDX) and patient-derived xenograft (PDX) model. These findings provide strong preclinical evidence supporting the therapeutic potential of VEN and ROCKi combination in AML.

Methods:

The *Online Supplementary Appendix* contains detailed information on experimental methods and materials.

Cell culture

AML cell lines and primary AML patient cells were cultured as previously described.[20] Cell lines were validated by short tandem repeats (STR) profiling (Genetica). See *Supplementary Appendix* for reagent details.

Clinical samples

Bone marrow aspirates or peripheral blood samples were obtained from AML patients after informed consent using protocols approved by the Institutional Review Board (IRB# 2000-186) of Penn State College of Medicine. Mutational profiling was performed as described previously.[21] See *Supplementary Appendix* for more details.

Cell viability assays and Synergy analysis

The cell viability of AML cells after combinatorial treatment was assessed by MTS assay.[18] The viability of primary AML patient cells was measured using CellTiter-Glo luminescence assay (Promega). The data was represented as % viability relative to vehicle control. The synergy between two drugs was analyzed using the SynergyFinder 2.0 web-application tool (https://synergyfinder.fimm.fi/).[22] See *Supplementary Appendix* for more details.

Assays and other methods

The details of colony-forming assay and other functional assays, including Annexin V staining, caspase-3/7 activity, reactive oxygen species (ROS) measurements, and mitochondrial membrane potential ($\Delta\Psi_m$) are provided in the *Supplementary Appendix*. Methods for assessing cellular respiration and $\Delta\Psi_m$ in intact cells are described in the *Supplementary Appendix*.

Immunoblotting analysis

The AML cell lines were left untreated or treated with DMSO (vehicle), GSK, VEN, and GSK+VEN combination at the indicated doses and time. Whole cell lysates were subjected to immunoblotting analysis with respective primary antibodies as described in the *Supplementary Appendix*.

***In vivo* mice efficacy and safety studies**

All animal studies were approved by the Institutional Animal Care and Use Committee (IACUC). The efficacy of GSK and VEN, alone and in combination, was evaluated in CDX and PDX models as described previously.[18,20] Short- and long-term safety studies were conducted, full experimental details of all *in vivo* studies are provided in the *Supplementary Appendix*.

Statistical analysis

Statistical tests were performed using GraphPad Prism 10 software. Results are presented as the mean ± standard error of the mean (SEM) or standard deviation (SD) from three independent experiments. A *p*-value of <0.05 (95% CI) is considered statistically significant. Comparisons between two groups were performed using a *t*-test, and comparisons among three or more groups were done by analysis of variance (ANOVA) with appropriate post hoc tests.

Results:

ROCK inhibitors synergize with VEN to induce potent anti-leukemic effects in AML cell lines *in vitro*

Since Rho/ROCK pathway genes were negatively enriched in the CRISPR loss-of-function screen with VEN (**Figure S1A, B**),[9] we performed correlation analysis to establish the relationship between VEN sensitivity (AUC-area under the curve) and normalized expression levels of Rho/ROCK pathway genes using the Beat AML dataset (http://vizome.org/aml2/inhibitor/).[23] The expression of Rho/ROCK pathway genes except *ROCK2* showed a positive correlation (higher expression linked to resistance) with VEN activity (**Figure S1C**). The positive correlation of *ROCK1* levels was comparable to that of *MCL1*, a well-known anti-apoptotic protein

associated with VEN resistance (**Figure S1D**). These findings support our hypothesis that suppressing ROCK activity can potentiate VEN-induced cytotoxicity in AML cells. To test the potential utility of ROCKi in combination with VEN, cytotoxicity assay was performed in VEN-sensitive and VEN-resistant AML cells, followed by Bliss analysis to assess the nature of the interaction. All the tested ROCKi (Fasudil, DJ4, and GSK269962A) exhibited strong synergistic cytotoxicity in combination with VEN in the VEN-sensitive AML cell lines (MV4-11, MOLM-13, HL-60, and OCI-AML2) tested (**Figure 1A**; **Table 1**). Inherently VEN-resistant (OCI-AML3, KG-1, and U937) or acquired VEN-resistant (MV4-11/VENR) AML cells exhibited at least additive (often synergistic) growth inhibition with the ROCKi and VEN combination (**Figure 1B**; **Table 1**). Representative dose-response matrices and corresponding Bliss synergy analysis for the ROCKi+VEN combination versus MV4-11 cells (naïve and VEN-resistant) are shown in **Figure 1 and S2**. These findings show that inhibition of ROCK activity significantly enhances VEN-induced cytotoxicity in both VEN-sensitive and VEN-resistant AML cells *in vitro.*

GSK269962A synergize with VEN to reduce leukemia burden in mice

We next assessed the *in vivo* efficacy of different ROCKi (Fasudil, DJ4, and GSK) in combination with VEN using a luciferase-labeled MV4-11 (sensitive to GSK and VEN) CDX model (**Figure 2A, Figure S3A**). Of the three ROCKi tested, GSK exhibited strong synergistic antileukemic activity in combination with VEN *in vivo*. Mice treated with both GSK (10mg/kg) and VEN (100mg/kg) for three weeks demonstrated a significantly lower leukemia burden compared to vehicle control (**Figure 2B, C**). Flow cytometric analysis of peripheral blood also revealed that mice treated with GSK+VEN combination had significantly lower burdens of circulating leukemia cells (hCD45+Ve) compared to vehicle control (**Figure 2D**). Moreover, mice treated with GSK+VEN combination showed significantly ($p<0.01$) higher overall median survival of 56 days, relative to the single agent (~45 days) and vehicle (38 days) groups (**Figure 2E**). Further testing of VEN (100 mg/kg) efficacy in combination with fasudil (25mg/kg) or DJ4 (10mg/kg) showed minimal or no advantage over single agents alone due to poor pharmacokinetics and resulted in early deaths due to off-target toxicity of fasudil and DJ4 (**Figure S3**). Given its ROCK selectivity, oral bioavailability, and apparent tolerability, most subsequent efforts were focused on the combination of GSK with VEN.

Next, this combination was tested in other CDX mouse models: MV4-11/VENR (acquired VEN resistance), MOLM-13 (inherently GSK resistant), and U937 (inherently resistant to both GSK and VEN) (**Figure 2, Table S1**). The MV4-11/VENR CDX mice treated with GSK+VEN combination showed significantly lower leukemia burden (**Figure 2F, G**) and prolonged overall median survival to 53 days from 49 days for vehicle and 44 days for VEN subjects (**Figure 2H**). Similarly, MOLM-13 CDX mice treated with the GSK (10mg/kg) and VEN (50mg/kg) combination showed a significantly lower leukemia burden (**Figure 2I; Figure S4A-B**) and increased overall survival to 24 days from 20 days for vehicle or GSK and 22 days for VEN subjects (**Figure 2J**). Flow cytometric analysis showed that GSK treatment alone is ineffective but can significantly lower the percentage of circulating leukemia cells in combination with VEN (**Figure 2I**). Lastly, we tested the effectiveness of GSK+VEN combination in the U937 CDX model. Similar to MOLM-13, U937 CDX is an aggressive leukemia model and showed a significantly lower leukemia burden after 2-weeks of treatment with the GSK (10mg/kg) and VEN (100mg/kg) combination (**Figure S4C, D**). Flow cytometric analysis of bone marrows revealed that GSK+VEN group exhibited lower engraftment levels compared to vehicle and single agent groups (**Figure 2K**). Altogether, our *in vivo* efficacy studies indicate that the selective ROCKi GSK potentiates VEN-mediated antileukemic activity in naïve and VEN-resistant (inherent or acquired) preclinical AML CDX mouse models.

VEN synergizes with GSK269962A against primary AML patient cells and cooperatively decreases leukemic burden in a patient-derived xenograft (PDX) mouse model

To validate cell line findings, we analyzed multiple primary AML patient samples with diverse genetic alterations. Bliss analysis revealed that more than 60% of the tested AML patient cells showed synergy with GSK+VEN combination, whereas the remaining cases exhibited additive responses (**Figure 3A, B; Figure S5; Table 2).** This effect shows no clear correlation with major AML subgroups (**Figure S6**). The addition of GSK to VEN significantly reduced clonogenicity of leukemic progenitor cells compared to single-agent treatments (**Figure 3C**). Assessment of GSK+VEN combination on normal cord-blood mononuclear cells (CB-MNCs) showed less inhibition of colony formation relative to AML patient cells (**Figure 3C**). These findings indicate that the GSK+VEN combination effectively exerts cytotoxicity in clinically relevant primary AML cells, inhibiting their clonogenicity while relatively sparing normal hematopoietic progenitors.

We next assessed the *in vivo* efficacy of GSK+VEN combination in a clinically relevant AML bioluminescent PDX mouse model (**Figure 4A**). A luciferase-labeled PDX model was generated to evaluate the combination therapy and monitor leukemia progression. Notably, the luciferase-labeled 1265 cells used for PDX injection (passage 2) exhibited mutation allele frequencies comparable to those of the primary cells (passage 0).[24] The treatment of 1265-Luc PDX mice with GSK (30mg/kg) and VEN (50mg/kg) combination resulted in a decreased leukemic burden compared to vehicle control (**Figure 4B, C**). Engraftment analysis by flow cytometry revealed that PDX mice treated with GSK+VEN combination exhibited a lower leukemia burden compared to vehicle group (**Figure 4D, E**). Notably, in the PDX study, two deaths were observed, one in the GSK group and one in the GSK+VEN group for unknown reasons. No deaths or treatment-related toxicity were observed across four CDX models treated for 2 to nearly 4 weeks, nor in the 2- and 4-week safety studies. The affected NRG-S mice appeared clinically normal, with stable bioluminescent signals and no gross abnormalities at necropsy. These results suggest that GSK+VEN combination provides superior antileukemic activity than VEN for the treatment of AML.

GSK, VEN, and their combination were well tolerated following short- and long-term exposure, with no observable signs of treatment-related toxicity

Although the GSK+VEN combination was well-tolerated across leukemia-bearing animal models, two deaths in the PDX study prompted dedicated short- and long-term safety evaluations. Normal Swiss Webster mice were treated for 2-weeks (short-term) or 4-weeks (long-term) with GSK (30 mg/kg) and VEN (50 or 100 mg/kg), alone or in combination (**Figure S7A; Figure S8A**). Body weight increased similarly across all groups, with no indication of treatment-related weight loss or overt clinical toxicity (**Figure S7B; Figure S8B**). Mild reductions in total white blood cell counts were noted but remained within normal limits; lymphopenia was restricted to the GSK+VEN group, whereas neutrophils, monocytes, erythrocyte indices, hemoglobin, and platelets were unchanged apart from the expected VEN-associated platelet increase (**Figure S7C; Figure S8C; Table S2**). Serum biochemical markers of liver and kidney function, electrolytes, metabolic parameters, and calcium also remained within the normal range with slight increases in blood glucose that remained within the normal range and mild elevations in liver enzymes (ALT and AST) that were not significantly different from controls (**Figure S7D-F; Figure S8D-F; Table S3**). Importantly, no deaths occurred in any treatment group during the 4-week

study, and no weight loss, clinical signs, or overt toxicity were observed. Collectively, these results demonstrate that the GSK+VEN combination is well tolerated with both short-term and extended repeated dosing.

GSK269962A treatment potentiates the VEN-induced mitochondrial depolarization, ROS levels, and apoptosis in AML cells

To test the effect of GSK on VEN-induced apoptosis, Annexin V/PI staining and caspase-3/7 activation were measured in both the parental and VEN-resistant MV4-11 cells. As expected, treatment with VEN or GSK alone exhibited dose-dependent caspase-3/7 activation and an increase in Annexin V-positive cells in both naïve and VENR cells (**Figure 5A-D**). The GSK+VEN combination resulted in significantly enhanced activation of Caspase-3/7 and Annexin V-positive cells in MV4-11 (**Figure 5A, C**) and MV4-11/VENR cells (**Figure 5B, D**) compared to VEN treatment. As VEN is known to inhibit mitochondrial respiration and alter mitochondrial outer membrane permeabilization (MOMP),[25] we investigated the effect of GSK co-treatment on VEN-induced $\Delta\Psi_m$ and the associated cellular ROS production. Both GSK and VEN, when used as single agents, exhibited a dose-dependent increase in mitochondrial depolarization and ROS in MV4-11 and MV4-11/VENR cells (**Figure 5E-H**). Interestingly, the GSK+VEN combination resulted in a significant increase in depolarized and ROS-positive MV4-11 (**Figures 5E, G**) and MV4-11/VENR (**Figure 5F, H**) cells compared to VEN treatment. These results indicate that GSK potentiates VEN-induced MOMP, thereby elevating ROS levels in AML cells to induce synergistic apoptosis. Although VEN inhibits mitochondrial respiration, AML cells have sustained $\Delta\Psi_m$ through ATP hydrolysis and developed resistance to therapy.[26] To measure $\Delta\Psi_m$ in intact cells, we measured TMRM (tetramethylrhodamine methyl ester) fluorescence after 15h and 24h of treatment. MV4-11 cells showed active voltage across the membrane with an increase in TMRM fluorescence (hyperpolarization) after 15h of treatment (single and combination), whereas 24h of treatment with GSK and GSK+VEN combination resulted in decreased TMRM fluorescence (depolarization) (**Figure 5I**). Similarly, MV4-11/VENR cells exhibited a biphasic response (hyperpolarization at 15h followed by normalization at 24h) with GSK treatment (**Figure 5J**). In line with our TMRM findings, the intact MV4-11/VENR cells treated with GSK exhibited higher maximal rate of respiration (**Figure 5K**). The oxidative phosphorylation (OXPHOS) capacity in permeabilized MV4-11/VENR cells indicated that GSK targets Complex IV (**Figure 5L**). The parental MV4-11 cells only exhibited synergistic effect on TMRM fluorescence (mitochondrial polarization) in viable intact cells very similar to that of activity

seen in bulk cells (**Figure 5G**) with GSK+VEN combination. The effects of GSK+VEN combination on mitochondrial polarization were suboptimal in both bulk (**Figure 5H**) and viable intact VENR cells (**Figure 5J**). These findings suggest that the combined effect of GSK and VEN is mediated by direct action on mitochondria that alter MOMP and increase ROS, ultimately leading to synergistic cytotoxicity in AML cells. Altogether, GSK+VEN combination effectively induces apoptosis through mitochondrial depolarization and elevated ROS levels in naïve and VEN-resistant AML cells.

GSK269962A treatment suppresses VEN-induced pro-survival proteins to promote apoptosis in AML cells

To investigate the mechanism of synergy between GSK and VEN in promoting apoptosis, we performed immunoblotting analyses in MV4-11 and MV4-11/VENR cells following treatment with GSK, VEN, or GSK+VEN combination. The levels of cleaved CASPASE-3 were dramatically increased with the combination treatment, consistent with a synergistic effect of GSK and VEN in inducing AML cell death (**Figure 6A**). Additionally, the steadily increased levels of cleaved PARP-1 (poly(ADP-ribose) polymerase-1), a known substrate for caspases, with combination treatment compared to single agents, suggest effective induction of apoptosis in both VEN-sensitive and VEN-resistant cells. The level of ROCK1 decreased with GSK treatment, consistent with the previous report,[19] and there was an increase in the shorter isoform of ROCK1 with the combination treatment. The level of ROCK2 appeared to be stable with a subtle decrease in the phosphorylated PTEN (phosphatase and tensin homolog) levels after the treatments.

As ROCK1 is known to undergo CASPASE-3-mediated cleavage,[27] the appearance of constitutively active cleaved-ROCK1 correlate with higher cellular apoptosis induced by combination treatment compared to single agents. As expected, treatment with ROCKi GSK resulted in lower levels of phosphorylated COFILIN, a downstream protein regulated by ROCK activation. Intriguingly, AML cells treated with VEN showed increased levels of phosphorylated COFILIN, which mimics the activation of ROCK1 independent of Rho activity via CASPASE-3-directed truncation.[27] However, the addition of GSK suppressed the VEN-mediated ROCK1 activation as indicated by decreased levels of phospho-COFILIN (the inactive form). The activation of COFILIN through dephosphorylation has been shown to result in its mitochondrial translocation, initiating intrinsic apoptosis by opening the mitochondrial permeability transition pore and subsequent release of cytochrome

c.[28,29] Thus, the COFILIN activation with GSK+VEN combination might be a crucial mechanism for the induction of mitochondrial apoptosis in both naïve and VEN-resistant AML cells.

Next, immunoblotting analysis of different BCL-2 family proteins showed that the addition of GSK suppressed the levels of phosphorylated BCL-2, a pro-survival protein induced by VEN in MV4-11 cells (**Figure 6A**). Moreover, the VEN-induced MCL1 (anti-apoptotic protein associated with VEN resistance) levels were suppressed by GSK addition in AML cells. The pro-apoptotic proteins such as NOXA and shorter isoforms of MCL1 (S-short & ES-extra short)[30,31] were increased with GSK+VEN combination compared to single-agent treatment and correlated with higher levels of caspase activity and apoptosis (**Figure 6A**). The upregulation of NOXA, a pro-apoptotic BCL-2 member that neutralizes MCL1 and other anti-apoptotic BCL-2 family proteins,[32] and the suppression of VEN-induced MCL1 levels by GSK imply a pro-apoptotic mechanism that contributes to synergistic cytotoxicity of GSK+VEN combination (**Figure 6A**). These effects were seen consistently in both the naïve and VEN-resistant MV4-11 AML cells.

Next, we tested the early dynamics of target protein expression by immunoblotting analysis. Interestingly, GSK+VEN combination resulted in the appearance of cleaved-PARP (apoptosis mediator) and executionary cleaved CASPASE-3 as early as 6h, with a gradual increase over 12h and 24h of treatment compared to single agents (**Figure 6B**). Accordingly, the cleaved ROCK1 levels were higher after 12h and 24h of GSK+VEN treatment compared to single agents alone. The cells treated with GSK+VEN exhibited upregulation of ROCK1/2, Dynamin-related protein 1 (DRP1), phosphorylated DRP1 (activation) and PTEN after 6h and 12h of treatment, with normalization after 24h of treatment. The increased levels of pro-apoptotic BAK after 6h and 12h of GSK+VEN treatment relative to single agents were consistent with synergistic apoptosis induction. Pro-apoptotic proteins, including NOXA and MCL1-ES, were also strongly upregulated following GSK+VEN combination compared to either agent alone. Although pro-survival BCL-2 members (BCL-2 and BCL-XL) were upregulated, MCL1 levels were suppressed after 24h of treatment with GSK and the GSK+VEN combination (**Figure 6B**). Overall, time-course immunoblotting analysis demonstrated that the GSK+VEN combination increases the expression of multiple apoptosis regulators and primes AML cells for cell death in a time-dependent manner. These findings indicate that GSK antagonizes pro-survival proteins induced by VEN, while

increasing pro-apoptotic proteins to synergistically induce cell death in both VEN-sensitive and VEN-resistant AML cells (**Figure 6C**).

Discussion:

In this study, we established a synergistic antileukemic interaction between BCL-2 and ROCK inhibitors in multiple preclinical AML models. VEN, a clinically approved and orally bioavailable BCL-2 inhibitor with a well-defined pharmacokinetic profile, provided a robust backbone for exploring such combinations, whereas GSK represents a newer, preclinical, orally available ROCK inhibitor. In AML pathogenesis, aberrant ROCK signaling has been linked to leukemic cell survival, drug resistance, and leukemic stem cell maintenance.[16,33] ROCKi has proven effective in AML and various solid tumors, highlighting the pathway's broader therapeutic significance.[34] All three structurally different ROCKi (DJ4, Fasudil, GSK) synergized with VEN in triggering cell death in AML cells *in vitro*. Nonetheless, while exhibiting *in vitro* synergistic action in conjunction with VEN, the preliminary *in vivo* trials of DJ4 and Fasudil co-administration with VEN revealed only moderate activity, attributable to dose-limiting toxicities and adverse pharmacokinetic properties. We focused on GSK, an orally bioavailable ROCKi that has enhanced selectivity and tolerability. GSK demonstrated significant anti-leukemic activity *in vivo* when administered in conjunction with VEN in multiple CDX models. All the tested primary AML patient cases with diverse genetic subtypes exhibited additive to synergistic cytotoxicity with GSK+VEN combination *ex vivo*. GSK+VEN combination showed a significant efficacy in PDX mouse model generated from primary AML patient cells. This novel combination was found to be safe in normal mice after 4-weeks of treatment with no significant changes in renal function, liver function, electrolytes, and albumin levels. Regarding the CBC, mild to moderate reduction in white blood cell counts was observed in the GSK+VEN combination group, particularly in neutrophils, lymphocytes, and monocytes, a common pattern seen with many clinically active anti-leukemia agents. Importantly, these changes remained within normal limits, and there were no clinical signs of infection during or after the treatment. Hemoglobin and platelet counts did not show any clinically or statistically meaningful changes. No deaths or treatment-related toxicity were observed across four CDX models treated for up to nearly 4 weeks or in dedicated two independent 2- and 4-week safety studies. The late deaths of two PDX animals treated with GSK may not have been due to the neoplasm,

and testing long-term toxicity of GSK+VEN combination is of interest prior to future clinical trials but beyond the immediate scope of this work.

Mechanistically, GSK triggered apoptosis characterized by caspase-3/7 activation and markedly increased VEN-induced cytotoxicity. Our findings suggest that mitochondrial depolarization and increased ROS production may contribute to the synergistic cytotoxicity of GSK and VEN in both naïve and VEN-resistant AML cells. AML cells demonstrate inherent deficiencies in OXPHOS, and the restoration of oxidative ATP generation (hyperpolarization) has proven to be significantly lethal.[35] We observed early mitochondrial hyperpolarization (TMRM fluorescence at 15 hours) and depolarization at 24h, suggesting a priming effect that enhances the susceptibility of leukemic cells to apoptosis. Many chemotherapeutics, including VEN, have been shown to disrupt respiration in AML cells.[36,37] VEN, a known OXPHOS inhibitor, has been shown to inhibit proton-pumping mitochondrial respiratory complexes (I/II/IV) to disrupt respiratory flux in AML cells.[37] Interestingly, GSK showed inhibitory activity on complex IV in VEN-resistant MV4-11 cells, contradicting higher basal and maximal respiration levels observed with GSK treatment. Recently, it has been demonstrated that ROCK kinases mediate metabolic adaptation of cancer cells, and co-inhibition of ROCK and OXPHOS resulted in synergistic anticancer activity.[38] Therefore, our findings support the existing literature and suggest further mechanistic studies to explore how GSK-mediated biphasic effects on respiration align with VEN activity to induce apoptosis in AML cells.

The coordinated activity of BCL-2 family proteins is crucial for determining cell fate and is the key regulator of mitochondrial apoptosis.[39] The clinical utility of VEN, a selective BCL-2 inhibitor, is limited due to adaptation of cells and development of resistance resulting from the overexpression of other antiapoptotic BCL-2 family members such as MCL1 and BCL-XL.[40,41] Simultaneous targeting of BCL-2, BCL-XL, and MCL1 has been shown to exhibit synergistic cytotoxicity and rescue resistance to VEN.[42,43] As a single agent, GSK has been shown to downregulate the expression of anti-apoptotic proteins, including Survivin, MCL1, and BCL-XL, in AML cells.[19] Accordingly, the addition of GSK suppressed VEN-induced overexpression of BCL-2 and MCL1, while the effect on BCL-XL was subtle. Additionally, we observed a significant upregulation of pro-apoptotic MCL1-S/ES isoforms and NOXA proteins with GSK+VEN combination in naïve and VEN-resistant AML cells. These shorter spliced variants of MCL1 are known to interact with unspliced MCL1 and promote

mitochondrial apoptosis.[30,44] MCL1-ES is a distinct BCL-2 family protein that induces mitochondrial apoptosis independent of BAX and BAK, whereas other conventional BCL-2 family physiology is dependent on BAX and/or BAK oligomerization to promote apoptosis.[31] Therefore, we assume that the GSK+VEN combination elicits a synergistic induction of apoptosis through the distinctive activation of interactions between BCL-2 members and primed VEN-resistant cells susceptible to VEN. It has been previously shown that the levels of NOXA, a BH3-only pro-death BCL-2 member that inhibits MCL1, determine the sensitivity to BH3 mimetics and apoptosis.[45,46] Consistent with other VEN-based combinations,[47,48] the synergy between GSK and VEN in AML cells may be attributed to the induction of NOXA levels. Binding of NOXA to MCL1 was known to induce proteasome-mediated degradation of MCL1.[49] We observe a negative correlation between NOXA and MCL1 levels to some extent following GSK+VEN combination. In parallel, GSK inhibited VEN-induced phospho-COFILIN (inactive) levels and thus might be facilitating translocation of active COFILIN to mitochondria and interact with DRP1 to promote MOMP and apoptosis.[28,29] Altogether, our data suggest that the GSK+VEN combination targets distinct mechanisms to promote synergistic apoptosis in AML cells. Though beyond the scope of this work, our findings support future mechanistic studies to unfold complex interactions between BCL-2 family members and other apoptosis mediators resulting from GSK+VEN combination.

While the evaluated ROCKi agents are not yet ready for clinical use, these results establish a foundation for future advances. Fasudil and DJ4 require intraperitoneal administration and exhibit suboptimal pharmacokinetic profiles, underscoring the need for reformulation to improve their bioavailability and overall clinical applicability. GSK is an orally bioavailable compound, yet its long-term safety profile to be fully defined. Notwithstanding these observations, our findings indicate that ROCK inhibition may enhance the effectiveness of VEN against leukemia while remaining tolerable, warranting further preclinical studies and potentially advancing to early-phase clinical trials.

References:

1. SEERExplorer: An interactive website for SEER cancer statistics. Available from: https://seer.cancer.gov/statistics-network/explorer/ Accessed on 2025 April 16.
2. Tomlinson B, de Lima M, Cogle CR, et al. Transplantation Referral Patterns for Patients with Newly Diagnosed Higher-Risk Myelodysplastic Syndromes and Acute Myeloid Leukemia at Academic and Community Sites in the Connect(R) Myeloid Disease Registry: Potential Barriers to Care. Transplant Cell Ther. 2023;29(7):460.e1-460.e9.
3. Shimony S, Stahl M, Stone RM. Acute Myeloid Leukemia: 2025 Update on Diagnosis, Risk-Stratification, and Management. Am J Hematol. 2025;100(5):860-891.
4. Kantarjian HM, DiNardo CD, Kadia TM, et al. Acute myeloid leukemia management and research in 2025. CA Cancer J Clin. 2025;75(1):46-67.
5. Brancati S, Gozzo L, Romano GL, et al. Venetoclax in Relapsed/Refractory Acute Myeloid Leukemia: Are Supporting Evidences Enough? Cancers (Basel). 2021;14(1):22.
6. DiNardo CD, Jonas BA, Pullarkat V, et al. Azacitidine and Venetoclax in Previously Untreated Acute Myeloid Leukemia. N Engl J Med. 2020;383(7):617-629.
7. Pratz KW, Jonas BA, Pullarkat V, et al. Long-term follow-up of VIALE-A: Venetoclax and azacitidine in chemotherapy-ineligible untreated acute myeloid leukemia. Am J Hematol. 2024;99(4):615-624.
8. Xu X, Liu R, He A, Wang F. Real-world results of venetoclax combined with hypomethylating agents in young adults with relapsed/refractory acute myeloid leukemia. Hematology. 2023;28(1):2265206.
9. Chen X, Glytsou C, Zhou H, et al. Targeting Mitochondrial Structure Sensitizes Acute Myeloid Leukemia to Venetoclax Treatment. Cancer Discov. 2019;9(7):890-909.
10. Wojtuszkiewicz A, Schuurhuis GJ, Kessler FL, et al. Exosomes Secreted by Apoptosis-Resistant Acute Myeloid Leukemia (AML) Blasts Harbor Regulatory Network Proteins Potentially Involved in Antagonism of Apoptosis. Mol Cell Proteomics. 2016;15(4):1281-1298.
11. Zhang Q, Riley-Gillis B, Han L, et al. Activation of RAS/MAPK pathway confers MCL-1 mediated acquired resistance to BCL-2 inhibitor venetoclax in acute myeloid leukemia. Signal Transduct Target Ther. 2022;7(1):51.
12. Yan M, Luo X, Han H, et al. ROCK2 increases drug resistance in acute myeloid leukemia via metabolic reprogramming and MAPK/PI3K/AKT signaling. Int Immunopharmacol. 2024;140:112897.
13. Wei L, Surma M, Shi S, Lambert-Cheatham N, Shi J. Novel Insights into the Roles of Rho Kinase in Cancer. Arch Immunol Ther Exp (Warsz). 2016;64(4):259-278.
14. Riento K, Ridley AJ. Rocks: multifunctional kinases in cell behaviour. Nat Rev Mol Cell Biol. 2003;4(6):446-456.
15. Rath N, Olson MF. Rho-associated kinases in tumorigenesis: re-considering ROCK inhibition for cancer therapy. EMBO Rep. 2012;13(10):900-908.
16. Mali RS, Ramdas B, Ma P, et al. Rho kinase regulates the survival and transformation of cells bearing oncogenic forms of KIT, FLT3, and BCR-ABL. Cancer Cell. 2011;20(3):357-369.
17. Wermke M, Camgoz A, Paszkowski-Rogacz M, et al. RNAi profiling of primary human AML cells identifies ROCK1 as a therapeutic target and nominates fasudil as an antileukemic drug. Blood. 2015;125(24):3760-3768.
18. Golla U, Ehudin MA, Annageldiyev C, et al. DJ4 Targets the Rho-Associated Protein Kinase Pathway and Attenuates Disease Progression in Preclinical Murine Models of Acute Myeloid Leukemia. Cancers (Basel). 2021;13(19):4889.

19. Pan T, Wang S, Feng H, et al. Preclinical evaluation of the ROCK1 inhibitor, GSK269962A, in acute myeloid leukemia. Front Pharmacol. 2022;13:1064470.
20. Annageldiyev C, Gowda K, Patel T, et al. The novel Isatin analog KS99 targets stemness markers in acute myeloid leukemia. Haematologica. 2020;105(3):687-696.
21. Patel JP, Gonen M, Figueroa ME, et al. Prognostic relevance of integrated genetic profiling in acute myeloid leukemia. N Engl J Med. 2012;366(12):1079-1089.
22. Ianevski A, Giri AK, Aittokallio T. SynergyFinder 2.0: visual analytics of multi-drug combination synergies. Nucleic Acids Res. 2020;48(W1):W488-W493.
23. Bottomly D, Long N, Schultz AR, et al. Integrative analysis of drug response and clinical outcome in acute myeloid leukemia. Cancer Cell. 2022;40(8):850-864.e9.
24. Annageldiyev C, Golla U, Patel S, et al. A defined culture model for ex vivo expansion of primary AML cells preserves leukemic stem cells and clonal architecture for functional and therapeutic studies. Blood. 2025;146(Supplement 1):3488.
25. Roca-Portoles A, Rodriguez-Blanco G, Sumpton D, et al. Venetoclax causes metabolic reprogramming independent of BCL-2 inhibition. Cell Death Dis. 2020;11(8):616.
26. Hagen JT, Montgomery MM, Aruleba RT, et al. Acute myeloid leukemia mitochondria hydrolyze ATP to support oxidative metabolism and resist chemotherapy. Sci Adv. 2025;11(15):eadu5511.
27. Sebbagh M, Renvoize C, Hamelin J, Riche N, Bertoglio J, Breard J. Caspase-3-mediated cleavage of ROCK I induces MLC phosphorylation and apoptotic membrane blebbing. Nat Cell Biol. 2001;3(4):346-352.
28. Hu J, Zhang H, Li J, et al. ROCK1 activation-mediated mitochondrial translocation of Drp1 and cofilin are required for arnidiol-induced mitochondrial fission and apoptosis. J Exp Clin Cancer Res. 2020;39(1):37.
29. Li GB, Cheng Q, Liu L, et al. Mitochondrial translocation of cofilin is required for allyl isothiocyanate-mediated cell death via ROCK1/PTEN/PI3K signaling pathway. Cell Commun Signal. 2013;11:50.
30. Bae J, Leo CP, Hsu SY, Hsueh AJ. MCL-1S, a splicing variant of the antiapoptotic BCL-2 family member MCL-1, encodes a proapoptotic protein possessing only the BH3 domain. J Biol Chem. 2000;275(33):25255-25261.
31. Kim JH, Bae J. MCL-1ES induces MCL-1L-dependent BAX- and BAK-independent mitochondrial apoptosis. PLoS One. 2013;8(11):e79626.
32. Gomez-Bougie P, Menoret E, Juin P, Dousset C, Pellat-Deceunynck C, Amiot M. Noxa controls Mule-dependent Mcl-1 ubiquitination through the regulation of the Mcl-1/USP9X interaction. Biochem Biophys Res Commun. 2011;413(3):460-464.
33. Mali RS, Kapur S, Kapur R. Role of Rho kinases in abnormal and normal hematopoiesis. Curr Opin Hematol. 2014;21(4):271-275.
34. Barcelo J, Samain R, Sanz-Moreno V. Preclinical to clinical utility of ROCK inhibitors in cancer. Trends Cancer. 2023;9(3):250-263.
35. Nelson MA, McLaughlin KL, Hagen JT, et al. Intrinsic OXPHOS limitations underlie cellular bioenergetics in leukemia. Elife. 2021;10:e63104.
36. Panina SB, Baran N, Brasil da Costa FH, Konopleva M, Kirienko NV. A mechanism for increased sensitivity of acute myeloid leukemia to mitotoxic drugs. Cell Death Dis. 2019;10(8):617.
37. Lagadinou ED, Sach A, Callahan K, et al. BCL-2 inhibition targets oxidative phosphorylation and selectively eradicates quiescent human leukemia stem cells. Cell Stem Cell. 2013;12(3):329-341.
38. Blazanin N, Liang X, Mahmud I, et al. Therapeutic modulation of ROCK overcomes metabolic adaptation of cancer cells to OXPHOS inhibition and drives synergistic anti-tumor activity. bioRxiv. 2024 Sep 20. doi: 10.1101/2024.09.16.613317 [preprint, not peer-reviewed]

39. Shamas-Din A, Kale J, Leber B, Andrews DW. Mechanisms of action of Bcl-2 family proteins. Cold Spring Harb Perspect Biol. 2013;5(4):a008714.
40. Liu J, Chen Y, Yu L, Yang L. Mechanisms of venetoclax resistance and solutions. Front Oncol. 2022;12:1005659.
41. Ong F, Kim K, Konopleva MY. Venetoclax resistance: mechanistic insights and future strategies. Cancer Drug Resist. 2022;5(2):380-400.
42. Ramsey HE, Fischer MA, Lee T, et al. A Novel MCL1 Inhibitor Combined with Venetoclax Rescues Venetoclax-Resistant Acute Myelogenous Leukemia. Cancer Discov. 2018;8(12):1566-1581.
43. Wichert MC, Fortner C, Niedermayer A, et al. The dual BCL-2 and BCL-XL inhibitor AZD4320 acts on-target and synergizes with MCL-1 inhibition in B-cell precursor ALL. Blood Adv. 2024;8(23):6035-6042.
44. Kim JH, Sim SH, Ha HJ, Ko JJ, Lee K, Bae J. MCL-1ES, a novel variant of MCL-1, associates with MCL-1L and induces mitochondrial cell death. FEBS Lett. 2009;583(17):2758-2764.
45. Nakajima W, Hicks MA, Tanaka N, Krystal GW, Harada H. Noxa determines localization and stability of MCL-1 and consequently ABT-737 sensitivity in small cell lung cancer. Cell Death Dis. 2014;5(2):e1052.
46. Mei Y, Xie C, Xie W, Tian X, Li M, Wu M. Noxa/Mcl-1 balance regulates susceptibility of cells to camptothecin-induced apoptosis. Neoplasia. 2007;9(10):871-881.
47. Jin S, Cojocari D, Purkal JJ, et al. 5-Azacitidine Induces NOXA to Prime AML Cells for Venetoclax-Mediated Apoptosis. Clin Cancer Res. 2020;26(13):3371-3383.
48. Cojocari D, Smith BN, Purkal JJ, et al. Pevonedistat and azacitidine upregulate NOXA (PMAIP1) to increase sensitivity to venetoclax in preclinical models of acute myeloid leukemia. Haematologica. 2022;107(4):825-835.
49. Czabotar PE, Lee EF, van Delft MF, et al. Structural insights into the degradation of Mcl-1 induced by BH3 domains. Proc Natl Acad Sci U S A. 2007;104(15):6217-6222.

Table 1: Bliss synergy scores for the ROCK inhibitors (DJ4, Fasudil, GSK) and VEN combination in AML cell lines.

Bliss synergy score*						
AML cell line	**VEN activity**	**DJ4 + VEN**	**Fasudil + VEN**	**GSK + VEN**	**Mutated genes**	**TP53 status**
MV4-11	Sensitive	15.89	12.24	13.49	FLT3-ITD, KMT2Ar, MLL-AF4	WT
MV4-11/VENR	Resistant	29.72	13.97	10.44	-	-
MOLM-13	Sensitive	10.91	12.62	10.52	FLT3-ITD, KMT2Ar	WT
HL-60	Sensitive	19.24	11.57	25.59	CDKN2A, NRAS	del
OCI-AML2	Sensitive	18.76	12.38	18.21	DNMT3A	WT
OCI-AML3	Resistant	18.69	12.81	-3.07	DNMT3A, NPM1, NRAS	WT
U937	Resistant	10.94	3.43	9.4	PTEN, PTPN11, WT1	Mut
KG-1	Resistant	22.32	14.5	7.81	NRAS	Mut

VENR: Venetoclax resistant; *<-10: Antagonistic; -10 to 10: Additive; >10: Synergistic

Table 2: Characteristics of primary AML patient cells are listed along with the corresponding Bliss synergy scores for GSK and VEN combination.

S.No.	Pt. ID.	Disease stage	Age	Gender	WBC (K/uL)	Blast (%)	Cytogenetics	Molecular data	Bliss synergy score
1	1259	Refractory	79	F	81.30	90.5	43,XX,add(2)(q31),del(2)(q11.2),3,del(5)(q13q33),add(6)(p23),add(6)(q21),add(7)(q11.2),add(14)(p11.2) add(14)\(p11.2),del(17)(p11.2),-20,-21[11]	TP53	28.23
2	215	Newly diagnosed	74	M	348.00	94.0	44,XY,add(9)(p13),-16,-17,+mar[cp3]	DNMT3A	19.15
3	1364	Newly diagnosed	76	M	168.00	85.0	46,XY,t(1;4)(q25;p16)?c[20]	NPM1, FLT3-ITD, DNMT3A	17.44
4	1244	Newly diagnosed	51	M	138.90	63.5	46,XY,t(3;5)(q25;q35)[20]	FLT3-ITD	17.24
5	1258	Refractory	59	F	18.24	11.0	43-44,X,der(X)t(X;9)(q22;q22),add(2)(q31),add(3)(p21),del(3)(q11.1),add(4)(p14),add(5)(q11.2),-7,+8,-10,11,add(12)(p11.2),add(14)(q22),-17,-17,der(18)t(17;18)(q11.2;q23),add(19)(q13.3),add(20)(q11.2),+1-3mar[cp17]/84-89,idemx2[cp3]	TP53	14.94
6	1256	Newly diagnosed	50	F	61.38	95.7	46,XX[20]	NPM1, FLT3-ITD, DNMT3A, IDH2	13.33
7	1284	Relapsed	68	F	55.00	93.0	47,XX,+13[18]/46,XX,t(7;15)(q34;q11.2),del(13)(q12q14)	DNMT3A, IDH2, NRAS, SRSF2, RUNX1, STAG2	13.14
8	1265	Newly diagnosed	74	M	217.36	96.0	46,XY,t(7;11)(p15;p15)[20]	HOXA9/NUP98 fusion, TP53, TET2, BLM	12.92
9	1279	Relapsed	57	M	80.40	88.0	46,XY[20]	NPM1, DNMT3A, IDH2, PTPN11	12.49
10	1006	Newly diagnosed	48	M	22.04	73.8	46,XY,add(5)(q31)[11]/46,XY[9]	TET2, CEBPA, IDH1, GATA2, NOTCH1	12.3
11	329	Newly diagnosed	72	F	41.90	75.0	45,XX,inv(3)(q21q26.2),-7 [20]	KRAS, CRLF2	11.75
12	1032	Relapsed	48	F	15.85	74.5	46,XX[20]	NPM1, FLT3-TKD, IDH1, DNMT3A	11.52
13	1361	Newly diagnosed	59	F	114.00	90.0	46,XX[20]	ASXL1, FLT3-ITD, WT1	9.03
14	1232	Relapsed	46	F	46.40	52.8	46,XX[20]	FLT3-ITD, TET2, CEBPA	8.79
15	1342	Refractory	27	M	139.70	86.0	45,X,-Y[20]	NPM1, TET2	8.66
16	1229	Relapsed	57	F	21.36	0.92	46,XX[20]	NRAS, KRAS, IDH1, DNMT3A, ASXL1, STAG2	7.63
17	1341	Newly diagnosed	83	M	201.00	89.0	46,XY,t(1;3)(p34.1;q27),t(2;18)(q31;q11.2),del(11)(p11.2p15)[20]	CBL, KIT	7.51
18	939	Newly diagnosed	45	F	364.58	93.8	46,XX[20]	FLT3-ITD, BCORL1, SMG1, WT1	5.33
19	1290	Newly diagnosed	74	M	99.07	61.0	46,XY[20]	ASXL1, DNMT3A, IDH1, KRAS, NRAS, RUNX1	4.66
20	1044	Newly diagnosed	70	M	36.40	63.8	46,XY,i(17)(q10)[12]/47,idem,+13[2]/47,XY,+mar[6]	ASXL1, SRSF2, CBL, APC, SETBP1	4.64
21	1240	Newly diagnosed	64	F	116.50	70.0	41,XX,-5,add(6)(q13),der(7;16)(p10;q10),-11,-16,-17,add(17)(p11.2),-18,add(21)(p11.2),add(22)(p11.2)[18]/46,XX[2]	NPM1 neg, FLT3 neg, and CEBPA neg. Others not tested	Used only in CFU Assay
22	1103	Newly diagnosed	41	F	247.25	86.0	46,XX[20]	PTPN11, FLT3-ITD, NOTCH1	

*Patient IDs in **shaded area** indicates the cells used for CFU assay

Figure legends:

Figure 1: ROCK inhibitors exhibit synergistic cytotoxicity with venetoclax combination in AML cell lines *in vitro*. A & B) Dose-response matrix showing the percent growth inhibition in MV4-11 (A) and MV4-11/VENR (B) cells along with Bliss synergy score after ROCKi and VEN combination treatment for 24h (DJ4, Fasudil) and 48h (GSK269962A-GSK). Bliss scores greater than 10 were considered synergistic. Representative data from at least three independent experiments are presented.

Figure 2: GSK and VEN combination synergistically decrease leukemia burden in AML cell line xenograft models. A) Schematic depicting the treatment plan in cell line-derived xenograft (CDX) mouse models. The NRG-S mice were intravenously injected with AML cells (MV4-11-YFP-Luc, MV4-11/VENR-GFP-Luc, MOLM13-YFP-Luc, and U937-Luc-tdTomato) and randomized into experimental groups (Vehicle, GSK, VEN, and GSK+VEN) based on BLI signals before the initiation of treatment. The leukemia progression was monitored through BLI imaging, flow cytometry, and survival analysis. B) Bioluminescence imaging of MV4-11-YFP-Luc CDX mice (n=5) at indicated days. C) The leukemia burden in the MV4-11-YFP-Luc mice was quantified in the terms of BLI signals and presented as average radiance (p/s/cm^2/sr). ***p<0.001, ****p<0.0001 by 2-way ANOVA (Tukey's multiple comparisons test). D) Flow cytometric analysis of peripheral blood (PB) from MV4-11-YFP-Luc CDX mice at 36 days post-engraftment to assess circulating human leukemic cells (% hCD45 positive cells). Data are presented as mean ± SEM (n=5). **p<0.01 by one-way ANOVA (Tukey's multiple comparisons test) compared to vehicle control. E) Kaplan-Meyer survival analysis of MV4-11-YFP-Luc CDX mice after treatment with GSK, VEN and GSK+VEN combination. **p<0.01 by Gehan-Breslow-Wilcoxon test (n=5). F) The MV4-11/VENR-GFP-Luc CDX mice (n=5) were monitored regularly by IVIS imaging at indicated days. G) The leukemia burden in the MV4-11/VENR-GFP-Luc CDX mice after treatment with GSK, VEN and GSK+VEN combination was quantified in the terms of BLI signals and presented as average radiance (p/s/cm^2/sr). **p<0.01, ****p<0.0001 by 2-way ANOVA (Tukey's multiple comparisons test). H) Kaplan-Meyer survival analysis of MV4-11/VENR CDX mice after treatment with GSK, VEN and GSK+VEN combination. *p<0.05 by Gehan-Breslow-Wilcoxon test indicates statistical significance compared to vehicle control. I) Flow cytometric analysis of peripheral blood (PB) collected from MOLM-13-YFP-Luc CDX mice after 20 days of post-engraftment for the detection of circulatory human leukemic cells (% hCD45 positive

cells). Data are presented as mean ± SEM (n=5-6). **p<0.01 by 1-way ANOVA (Tukey's multiple comparisons test) compared to GSK. J) Kaplan-Meyer survival analysis of MOLM-13-YFP-Luc CDX mice after treatment with GSK, VEN and GSK+VEN combination. **p<0.01, ***p<0.001 by Gehan-Breslow-Wilcoxon test (n=5-6). K) Flow cytometric analysis of BM cells collected from U937-Luc-tdTomato engrafted CDX mice after 21 days of post-transplant for the detection of human leukemic cells (% tdTomato and hCD45 positive cells). Data are presented as mean ± SEM (n=4-5).

Figure 3: GSK and VEN combination inhibit the growth and clonogenicity of primary AML patient cells. A) Bliss synergy scores for AML patient cells (n=20) after 48h of treatment with GSK and VEN combination. The cell viability of patient cells was measured by the CellTiter-Glo assay. Bliss scores greater than 10 indicate 'synergy,' and 0-10 indicate 'additive' activity. B) Dose-response matrix showing the percent growth inhibition in three different primary AML patient cells (VEN-sensitive and VEN-resistant) along with Bliss synergy score after GSK and VEN combination treatment. C) Clonogenicity of the primary AML samples in the presence of either 0.5µM VEN, GSK (0.25-2.5µM), or GSK+VEN combination presented as % colonies relative to the vehicle (DMSO) control. Cord-blood mononuclear cells (CB-MNCs) were used as a normal control (n=1). The data are presented as mean ± SD (n=6) for AML patient cells and analyzed by two-way ANOVA (Tukey's multiple comparisons test) to compare the mean % colonies. *p<0.05, **p<0.01, ***p<0.001, **** p < 0.0001 indicate statistical significance.

Figure 4: Combination of GSK and venetoclax reduce the leukemia burden in AML PDX model. A) Schematic showing the generation of luc-labeled PDX mouse model using primary AML patient cells (Pt.1265). The primary 1265 patient cells were transduced overnight with a lentiviral vector expressing EGFP and luciferase (LUC2) genes. Unsorted cells (p^0-passage 0) after 24h of transduction were injected into NRG-S mice. GFP-sorted bone marrow cells harvested from primary PDX (P^1-passage 1) mice on day-147 post-transplant were cultured ex vivo for 12 days prior to injection into secondary recipients (P^2-passage 2). B) The bone marrow cells from secondary recipient mice (P^2) were injected intravenously into NRG-S mice at 0.6 million/mice (P^3-passage 3). The mice were randomized into four experimental groups (vehicle, GSK, VEN, GSK+VEN combo) of 5-7 mice each based on BLI signals after day 13 post-transplant. The mice were treated with GSK (30mg/kg, p.o., Mon-Sat), VEN (50 mg/kg, p.o., Mon-Sat), and GSK+VEN combination for three

weeks and monitored for leukemia burden through regular IVIS imaging. C) The BLI signals were quantified, and leukemia burden was represented in terms of average radiance (p/s/cm^2/sr). D) Flow analysis of bone marrow (BM) cells from 1265-luc PDX mice quantified engraftment of human CD45 positive cells or GFP positive cells. Data are presented as mean ± SEM (n=3-6) and analyzed by 2-way ANOVA (Tukey's multiple comparisons test). ***p<0.005 and ****p<0.0001 indicate statistical significance compared to vehicle control. E) A representative density plots showing the relative percent populations of hCD45 and EGFP positive cells in the BM cells collected from the experimental PDX mice groups.

Figure 5: GSK potentiate venetoclax-induced apoptosis, ROS and mitochondrial membrane depolarization in AML cells. Measurement of Annexin V levels (A & B), caspase-3/7 activity (C & D), ROS levels (E & F), and mitochondrial membrane depolarization levels (G & H) in MV4-11 and MV4-11/VENR cells after 48h of treatment with vehicle, GSK, VEN, and GSK+VEN combination. Data are presented as mean ± SD (n=3) and analyzed by 2-way ANOVA (Tukey's multiple comparisons test). I & J) Flow cytometric analysis of intact cell ΔΨm in MV4-11 (I) and MV4-11/VENR (J) cell lines after 15 and 24h of treatment. Data expressed as a percentage of maximal TMRM fluorescence relative to vehicle. Data are presented as mean ± SEM (n=3) and analyzed by 2-way ANOVA (Dunnett's multiple comparisons test). K & L) Measurement of OXPHOS capacity in intact (K) and permeabilized cells after 14h of treatment. Data are presented as mean ± SEM (n=3) and analyzed by 2-way ANOVA (Sidak's multiple comparisons test). *p<0.05, **p<0.01, ***p<0.005, ****p<0.0001 indicates statistical significance.

Figure 6: GSK suppresses pro-survival signaling induced by venetoclax to induce apoptosis in AML cells. A) Immunoblotting analysis of MV4-11 and MV4-11/VENR cells after 48h of treatment with vehicle and indicated doses of GSK (G), VEN (V), or both GSK and VEN. The levels of phospho-Cofilin (pCofilin), Mcl1 (anti-apoptotic), Noxa (pro-apoptotic), and cleaved caspase-3 (cCaspase-3) were quantified relative to GAPDH and normalized to untreated control cells. Mcl1 (S) and Mcl1 (ES) represent the "short (S)" and "extra short (ES)" isoforms that exhibit pro-apoptotic activity. GAPDH and β-Actin levels were used as loading controls. Representative blots from three independent experiments are shown. B) Immunoblotting analysis of MV4-11 cells after 6, 12, and 24h of treatment either with vehicle (DMSO-D), GSK-100nM (G), VEN-20nM (V), or GSK+VEN combination (C). GAPDH and β-Actin levels were used as loading controls. Representative blots

from two replicates are shown. C) Proposed mechanisms of action of GSK in combination with VEN. Inhibition of rho-kinases (ROCK1/2) with GSK increases active cofilin levels, leading to actin depolymerization and F-actin destabilization, which promote apoptotic pathways and impair cell contractility, adhesion, and invasion. Active cofilin (dephosphorylated) is known to translocate to mitochondria in complex with Drp1, where it promotes intrinsic apoptosis through mitochondrial outer membrane permeabilization (MOMP). Inhibition of anti-apoptotic Bcl-2 with VEN increases the activity of pro-apoptotic BH-3 only proteins like Noxa and facilitates Bax or Bak oligomerization, triggering MOMP and apoptosis. Treatment with GSK results in downregulation of anti-apoptotic proteins (BCL-2, MCL1) and upregulation of Noxa, further enhancing cell susceptibility to VEN. Also, GSK inhibits ROCK activation induced by VEN via caspase-mediated cleavage, leading to accumulation of apoptotic signals and more cell death. The artworks were adopted from Servier Medical Art (https://smart.servier.com/), licensed under a Creative Commons Attribution 4.0 Unported License.

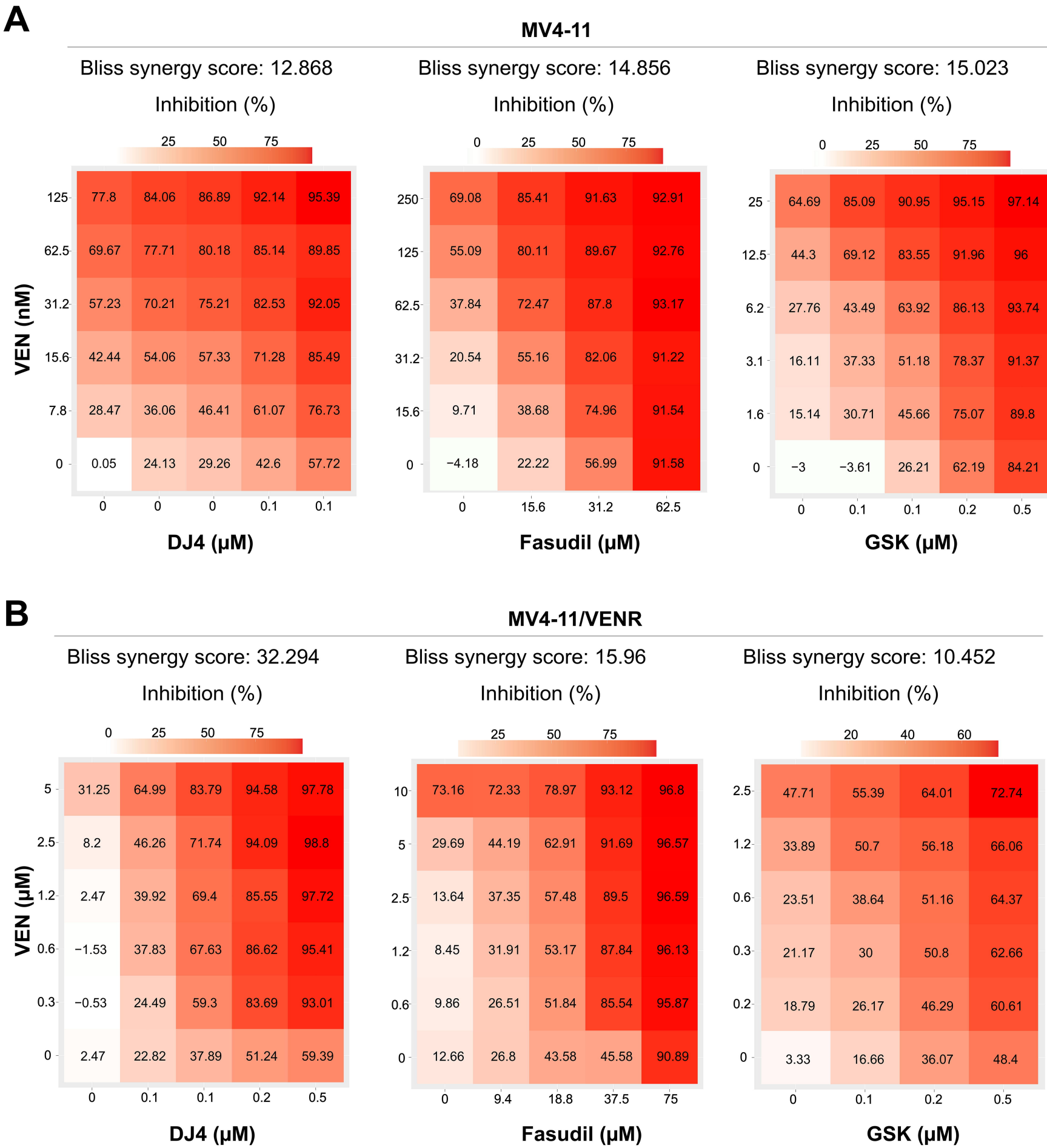
A
MV4-11
Bliss synergy score: 12.868
Inhibition (%)
25 50 75
VEN (nM)
125 77.8 84.06 86.89 92.14 95.39
62.5 69.67 77.71 80.18 85.14 89.85
31.2 57.23 70.21 75.21 82.53 92.05
15.6 42.44 54.06 57.33 71.28 85.49
7.8 28.47 36.06 46.41 61.07 76.73
0 0.05 24.13 29.26 42.6 57.72
0 0 0 0.1 0.1
DJ4 (μM)
Bliss synergy score: 14.856
Inhibition (%)
0 25 50 75
250 69.08 85.41 91.63 92.91
125 55.09 80.11 89.67 92.76
62.5 37.84 72.47 87.8 93.17
31.2 20.54 55.16 82.06 91.22
15.6 9.71 38.68 74.96 91.54
0 −4.18 22.22 56.99 91.58
0 15.6 31.2 62.5
Fasudil (μM)
Bliss synergy score: 15.023
Inhibition (%)
0 25 50 75
25 64.69 85.09 90.95 95.15 97.14
12.5 44.3 69.12 83.55 91.96 96
6.2 27.76 43.49 63.92 86.13 93.74
3.1 16.11 37.33 51.18 78.37 91.37
1.6 15.14 30.71 45.66 75.07 89.8
0 −3 −3.61 26.21 62.19 84.21
0 0.1 0.1 0.2 0.5
GSK (μM)
B
MV4-11/VENR
Bliss synergy score: 32.294
Inhibition (%)
0 25 50 75
VEN (μM)
5 31.25 64.99 83.79 94.58 97.78
2.5 8.2 46.26 71.74 94.09 98.8
1.2 2.47 39.92 69.4 85.55 97.72
0.6 −1.53 37.83 67.63 86.62 95.41
0.3 −0.53 24.49 59.3 83.69 93.01
0 2.47 22.82 37.89 51.24 59.39
0 0.1 0.1 0.2 0.5
DJ4 (μM)
Bliss synergy score: 15.96
Inhibition (%)
25 50 75
10 73.16 72.33 78.97 93.12 96.8
5 29.69 44.19 62.91 91.69 96.57
2.5 13.64 37.35 57.48 89.5 96.59
1.2 8.45 31.91 53.17 87.84 96.13
0.6 9.86 26.51 51.84 85.54 95.87
0 12.66 26.8 43.58 45.58 90.89
0 9.4 18.8 37.5 75
Fasudil (μM)
Bliss synergy score: 10.452
Inhibition (%)
20 40 60
2.5 47.71 55.39 64.01 72.74
1.2 33.89 50.7 56.18 66.06
0.6 23.51 38.64 51.16 64.37
0.3 21.17 30 50.8 62.66
0.2 18.79 26.17 46.29 60.61
0 3.33 16.66 36.07 48.4
0 0.1 0.2 0.5
GSK (μM)

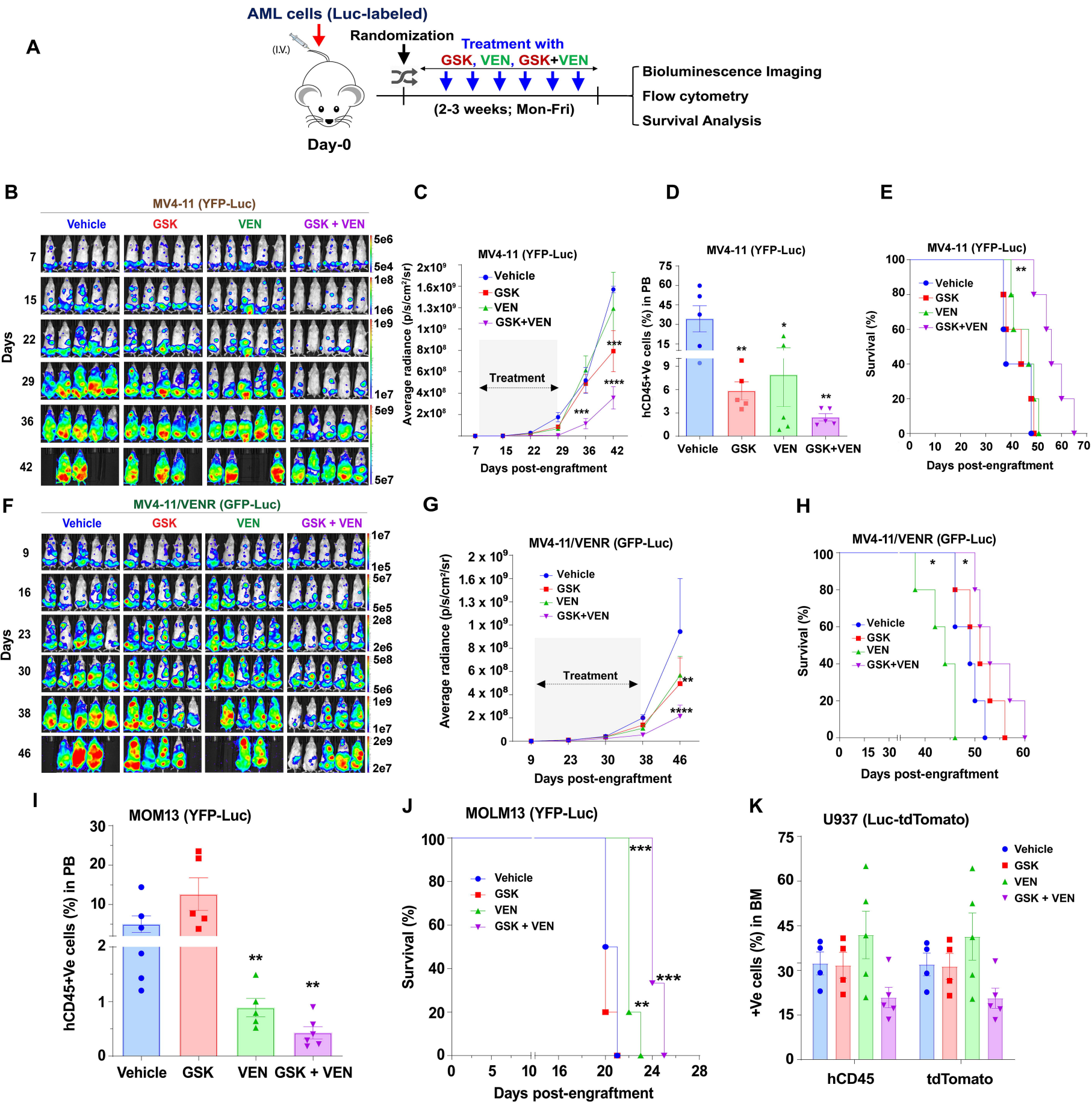
A
AML cells (Luc-labeled)
(I.V.)
Randomization
Treatment with
GSK, VEN, GSK+VEN
(2-3 weeks; Mon-Fri)
Bioluminescence Imaging
Flow cytometry
Survival Analysis
Day-0
B
MV4-11 (YFP-Luc)
Vehicle
GSK
VEN
GSK + VEN
Days
C
MV4-11 (YFP-Luc)
Average radiance (p/s/cm²/sr)
Vehicle
GSK
VEN
GSK+VEN
Treatment
Days post-engraftment
D
MV4-11 (YFP-Luc)
hCD45+Ve cells (%) in PB
E
MV4-11 (YFP-Luc)
Survival (%)
Days post-engraftment
F
MV4-11/VENR (GFP-Luc)
G
MV4-11/VENR (GFP-Luc)
H
MV4-11/VENR (GFP-Luc)
I
MOM13 (YFP-Luc)
J
MOLM13 (YFP-Luc)
K
U937 (Luc-tdTomato)
+Ve cells (%) in BM
hCD45
tdTomato

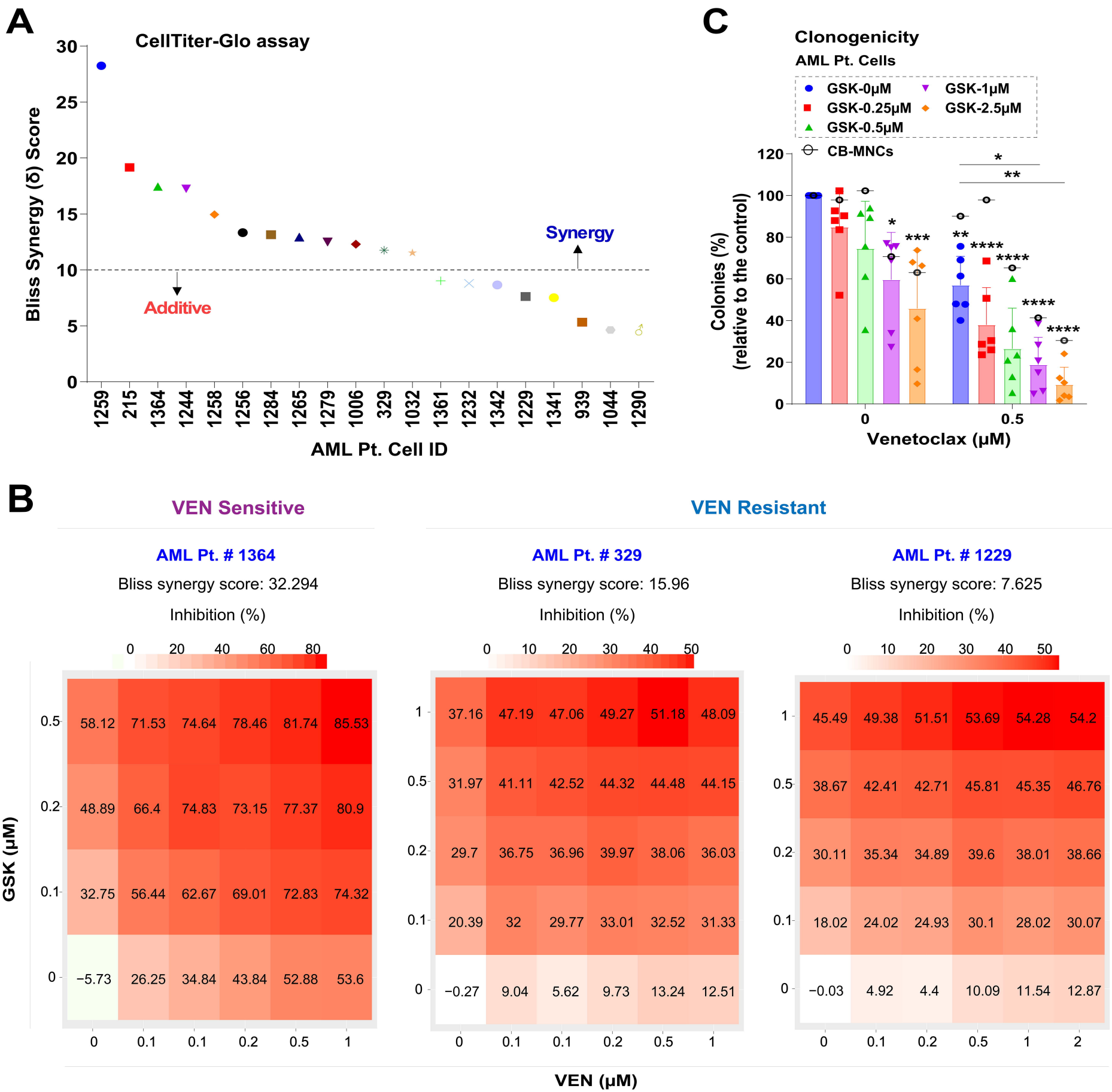
A
CellTiter-Glo assay
Bliss Synergy (δ) Score
Synergy
Additive
AML Pt. Cell ID
1259 215 1364 1244 1258 1256 1284 1265 1279 1006 329 1032 1361 1232 1342 1229 1341 939 1044 1290
C
Clonogenicity
AML Pt. Cells
GSK-0μM
GSK-0.25μM
GSK-0.5μM
GSK-1μM
GSK-2.5μM
CB-MNCs
Colonies (%)
(relative to the control)
Venetoclax (μM)
B
VEN Sensitive
VEN Resistant
AML Pt. # 1364
Bliss synergy score: 32.294
AML Pt. # 329
Bliss synergy score: 15.96
AML Pt. # 1229
Bliss synergy score: 7.625
Inhibition (%)
GSK (μM)
VEN (μM)

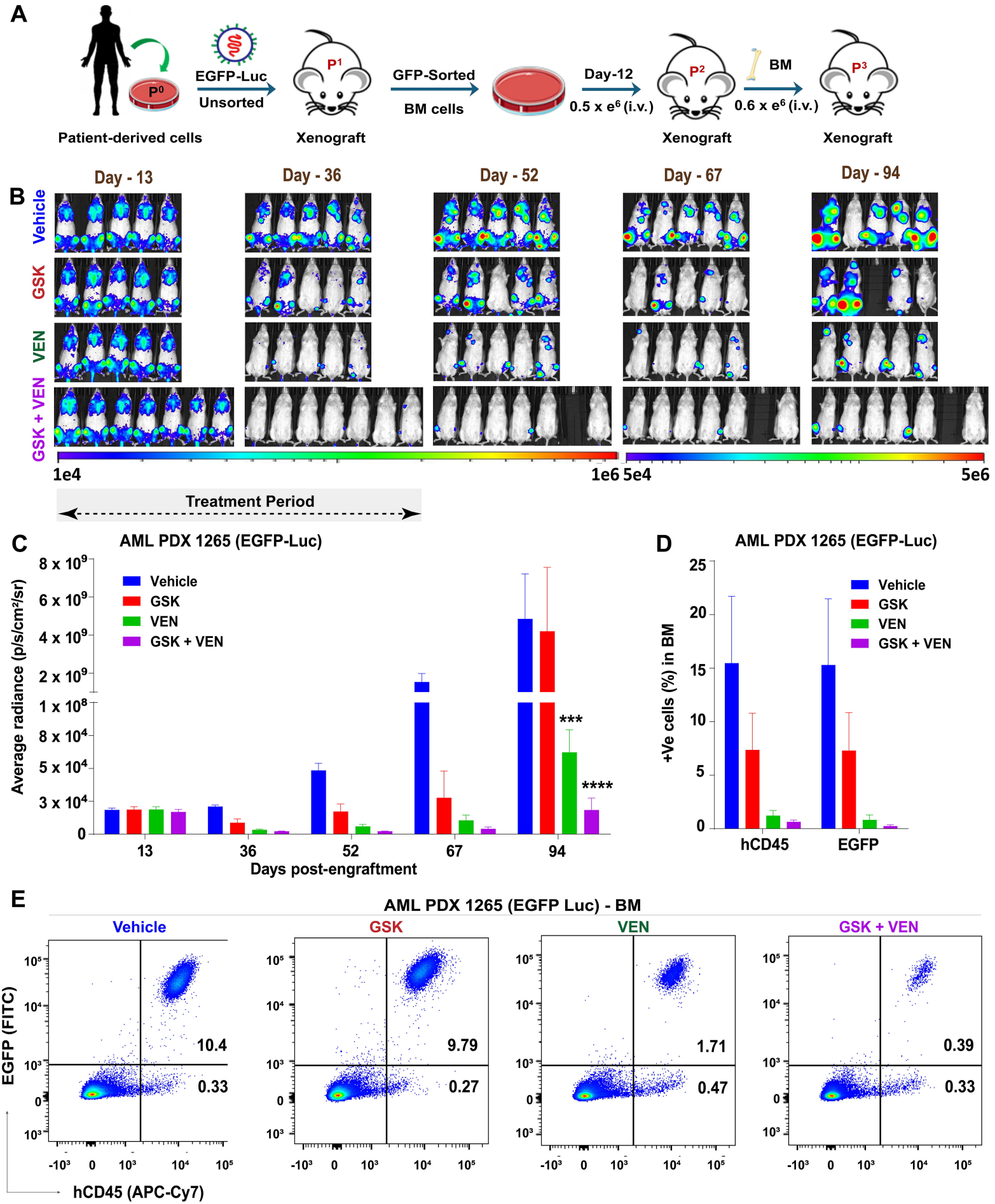
A
P0
EGFP-Luc
Unsorted
P1
GFP-Sorted
BM cells
Day-12
0.5 x e6 (i.v.)
P2
BM
0.6 x e6 (i.v.)
P3
Patient-derived cells
Xenograft
Xenograft
Xenograft
B
Day - 13
Day - 36
Day - 52
Day - 67
Day - 94
Vehicle
GSK
VEN
GSK + VEN
1e4
1e6
5e4
5e6
Treatment Period
C
AML PDX 1265 (EGFP-Luc)
Average radiance (p/s/cm²/sr)
8 x 10^9
6 x 10^9
4 x 10^9
2 x 10^9
1 x 10^8
8 x 10^4
5 x 10^4
3 x 10^4
0
Vehicle
GSK
VEN
GSK + VEN
***
****
13
36
52
67
94
Days post-engraftment
D
AML PDX 1265 (EGFP-Luc)
+Ve cells (%) in BM
25
20
15
10
5
0
Vehicle
GSK
VEN
GSK + VEN
hCD45
EGFP
E
AML PDX 1265 (EGFP Luc) - BM
Vehicle
GSK
VEN
GSK + VEN
EGFP (FITC)
hCD45 (APC-Cy7)
10.4
0.33
9.79
0.27
1.71
0.47
0.39
0.33

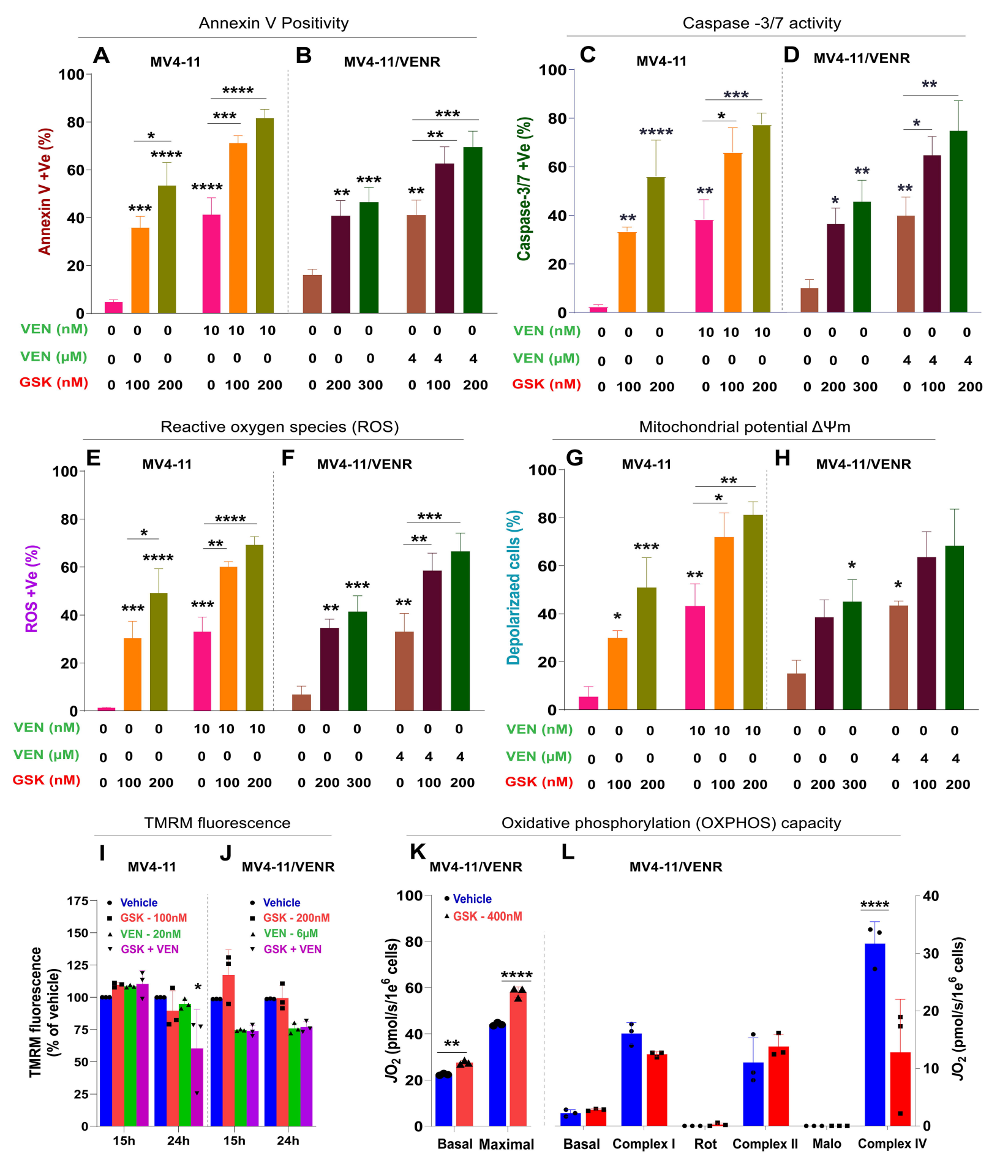
Annexin V Positivity
A
MV4-11
B
MV4-11/VENR
Annexin V +Ve (%)
Caspase -3/7 activity
C
MV4-11
D
MV4-11/VENR
Caspase-3/7 +Ve (%)
VEN (nM) 0 0 0 10 10 10 0 0 0 0 0 0
VEN (μM) 0 0 0 0 0 0 0 0 0 4 4 4
GSK (nM) 0 100 200 0 100 200 0 200 300 0 100 200
Reactive oxygen species (ROS)
E
MV4-11
F
MV4-11/VENR
ROS +Ve (%)
Mitochondrial potential ΔΨm
G
MV4-11
H
MV4-11/VENR
Depolarizaed cells (%)
TMRM fluorescence
I
MV4-11
J
MV4-11/VENR
Vehicle
GSK - 100nM
VEN - 20nM
GSK + VEN
GSK - 200nM
VEN - 6μM
TMRM fluorescence (% of vehicle)
15h
24h
Oxidative phosphorylation (OXPHOS) capacity
K
MV4-11/VENR
L
MV4-11/VENR
GSK - 400nM
JO2 (pmol/s/1e6 cells)
Basal
Maximal
Complex I
Rot
Complex II
Malo
Complex IV

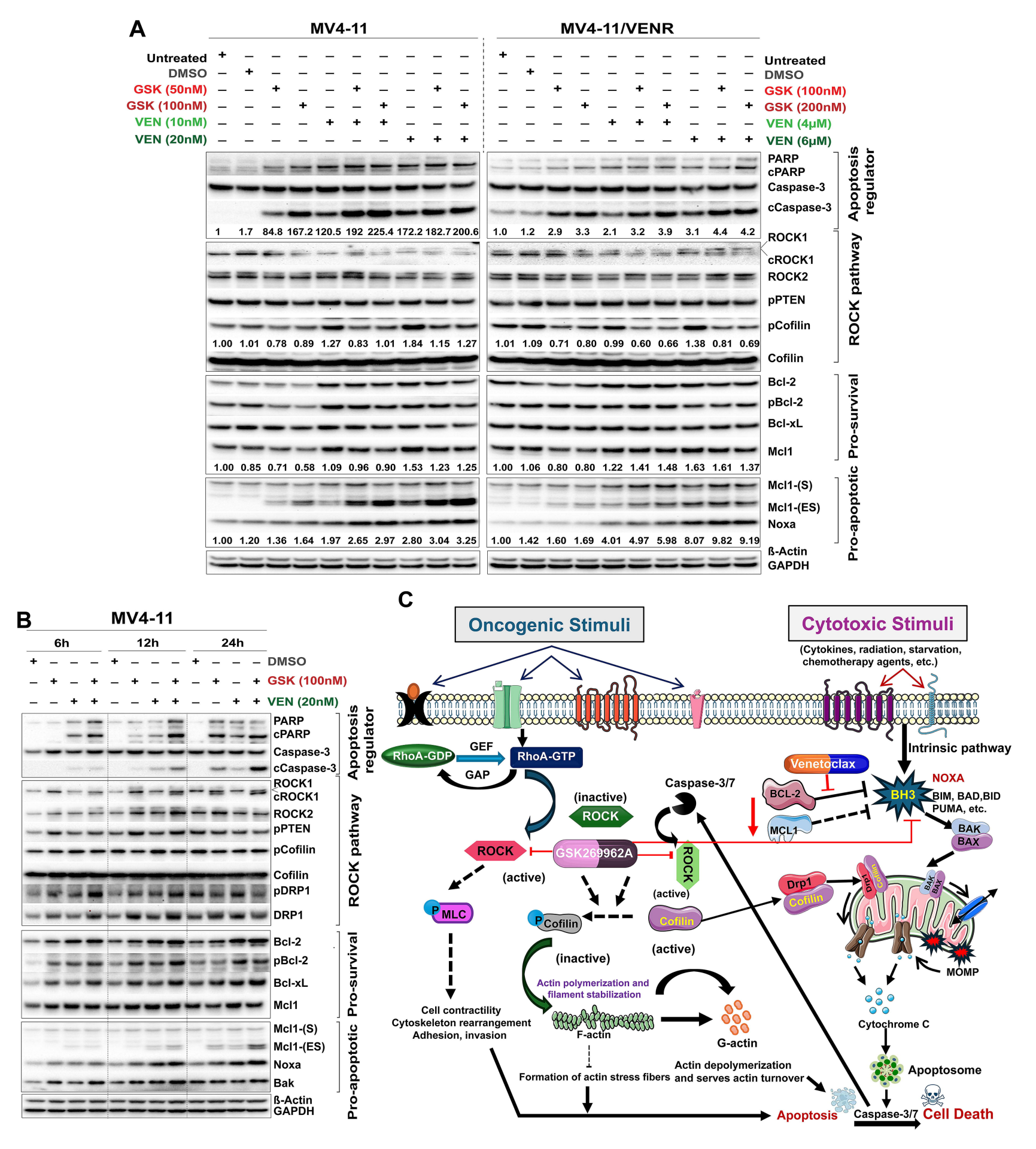
A
MV4-11
MV4-11/VENR
Untreated
DMSO
GSK (50nM)
GSK (100nM)
VEN (10nM)
VEN (20nM)
GSK (100nM)
GSK (200nM)
VEN (4μM)
VEN (6μM)
PARP
cPARP
Caspase-3
cCaspase-3
Apoptosis regulator
1 1.7 84.8 167.2 120.5 192 225.4 172.2 182.7 200.6
1.0 1.2 2.9 3.3 2.1 3.2 3.9 3.1 4.4 4.2
ROCK1
cROCK1
ROCK2
pPTEN
pCofilin
Cofilin
ROCK pathway
1.00 1.01 0.78 0.89 1.27 0.83 1.01 1.84 1.15 1.27
1.01 1.09 0.71 0.80 0.99 0.60 0.66 1.38 0.81 0.69
Bcl-2
pBcl-2
Bcl-xL
Mcl1
Pro-survival
1.00 0.85 0.71 0.58 1.09 0.96 0.90 1.53 1.23 1.25
1.00 1.06 0.80 0.80 1.22 1.41 1.48 1.63 1.61 1.37
Mcl1-(S)
Mcl1-(ES)
Noxa
Pro-apoptotic
1.00 1.20 1.36 1.64 1.97 2.65 2.97 2.80 3.04 3.25
1.00 1.42 1.60 1.69 4.01 4.97 5.98 8.07 9.82 9.19
ß-Actin
GAPDH
B
MV4-11
6h
12h
24h
DMSO
GSK (100nM)
VEN (20nM)
PARP
cPARP
Caspase-3
cCaspase-3
Apoptosis regulator
ROCK1
cROCK1
ROCK2
pPTEN
pCofilin
Cofilin
pDRP1
DRP1
ROCK pathway
Bcl-2
pBcl-2
Bcl-xL
Mcl1
Pro-survival
Mcl1-(S)
Mcl1-(ES)
Noxa
Bak
Pro-apoptotic
ß-Actin
GAPDH
C
Oncogenic Stimuli
Cytotoxic Stimuli
(Cytokines, radiation, starvation, chemotherapy agents, etc.)
Intrinsic pathway
RhoA-GDP
GEF
GAP
RhoA-GTP
(inactive)
ROCK
ROCK
(active)
GSK269962A
ROCK
(active)
Caspase-3/7
Venetoclax
BCL-2
MCL1
BH3
NOXA
BIM, BAD,BID
PUMA, etc.
BAK
BAX
Drp1
Cofilin
MOMP
Cytochrome C
Apoptosome
P MLC
P Cofilin
Cofilin
(active)
(inactive)
Actin polymerization and filament stabilization
F-actin
G-actin
Cell contractility
Cytoskeleton rearrangement
Adhesion, invasion
Formation of actin stress fibers
Actin depolymerization and serves actin turnover
Apoptosis
Caspase-3/7
Cell Death

Supplementary Appendix:

Title: Pharmacological blockade of rho kinase enhances venetoclax responses in translational models of acute myeloid leukemia

Running Title: Targeting ROCK improves venetoclax response in AML

Author List and Affiliations:

Upendarrao Golla[1], Riya Bhalodia[2,†], Charyguly Annageldiyev[1], Satyam Patel[2], Vishnu Sravan Bollu[1,2], Su-Fern Tan[3,4], Myles C. Cabot[4], David J. Feith[3,4], Thomas P. Loughran Jr.[3,4], Ross L. Levine[5,6], Shin Mineishi[1], Hong Zheng[1], Kentaro Minagawa[1], Jeremy Hengst[7], Giselle L. Saulnier Sholler[7], Dhimant Desai[2,8], Sinisa Dovat[7], Kelsey H. Fisher-Wellman[9], David F. Claxton[1,8], Arati Sharma[2,8,#]

[1]Division of Hematology and Oncology, Department of Medicine, Pennsylvania State University College of Medicine, Hershey, PA, USA

[2]Department of Molecular and Precision Medicine, Pennsylvania State University College of Medicine, Hershey, PA, USA

[3]Department of Medicine, Division of Hematology & Oncology, University of Virginia School of Medicine, Charlottesville, VA, USA

[4]University of Virginia Comprehensive Cancer Center, Charlottesville, VA, USA

[5]Human Oncology and Pathogenesis Program, Memorial Sloan Kettering Cancer Center, New York, NY, USA

[6]Leukemia Service, Department of Medicine and Center for Hematologic Malignancies, Memorial Sloan Kettering Cancer Center, New York, NY, USA

[7]Division of Hematology and Oncology, Department of Pediatrics, Pennsylvania State University, College of Medicine, Hershey, PA, USA

[8]Penn State Cancer Institute, Pennsylvania State University College of Medicine, Hershey, PA, USA

[9]Department of Cancer Biology, Atrium Health Wake Forest Baptist Comprehensive Cancer, Wake Forest University School of Medicine, Winston-Salem, NC, USA

[†]Current address: Saint Louis University School of Medicine, Saint Louis, MO, USA

[#]Corresponding Author:

Arati Sharma, Ph.D.

Department of Molecular and Precision Medicine, Pennsylvania State University College of Medicine, Hershey, PA 17033

Phone: 717-531-0003 (ext. 289551); E-mail: asharma@pennstatehealth.psu.edu

Materials and Methods:

Materials

DJ4 was synthesized at the Organic Synthesis Core (RRID:SCR_012425) of the Penn State College of Medicine, as reported previously.[1] Fasudil (Cat# A702414), GSK269962A (Cat# A266066), and venetoclax (Cat# A156386) were procured from AmBeed (Buffalo Grove, IL, USA). The cytokines stem cell factor (SCF; #100-04), FLT3 ligand (FLT3-L; #100-21AF), and GM-CSF (#100-08) were purchased from FUJIFILM Irvine Scientific (Santa Ana, CA). Interleukin-3 (IL-3; #203-IL) was obtained from R&D Systems (Minneapolis, MN), and granulocyte colony-stimulating factor (G-CSF; Neupogen®) was obtained from the pharmacy. StemRegenin1 (SR1; # S2858) was purchased from Selleckchem (Houston, TX). Lentiviral vector pLV-EF1a-LUC2-T2A-EGFP was procured from VectorBuilder (Chicago, IL, USA). All other reagents used were of molecular biology grade.

Clinical samples

Bone marrow aspirates or peripheral blood samples were obtained from AML patients during diagnosis or disease relapse after informed consent using protocols approved by the Institutional Review Board (IRB# 2000-186) of the Penn State College of Medicine. Cord blood (CB) samples were obtained from freshly delivered placentas of healthy donors at Penn State Health Obstetrics and Gynecology. Mononuclear cells (MNCs) were isolated through density gradient separation (Ficol-Paque, GE Healthcare Life Sciences, Pittsburgh, PA).

Cell culture

AML cell lines were cultured in either RPMI-1640 (#10-040; for MOLM-13, OCI-AML2, OCI-AML3, and U937) or IMDM (#10-016; for MV4-11, MV4-11/VENR, HL-60, and KG-1) growth media (Corning, NY, USA) supplemented with 10% heat-inactivated fetal bovine serum (FBS) (ThermoFisher Scientific, USA; #A5209502) and 1X Penicillin-Streptomycin (GIBCO, Gaithersburg, MD) at 37°C in a humified incubator with 5% CO_2. AML cell lines HL-60 (#CCL-240, CVCL_0002), KG-1 (#CCL-246, RRID:CVCL_0374), and MV4-11 (#CRL-9591, RRID: CVCL_0064) were obtained from the American Type Culture Collection (ATCC) (Manassas, VA, USA). VEN-resistant MV4-11 cells (MV4-11/VENR) were generated via continued subculture in increasing doses of VEN, beginning at 2nM and doubling until reaching a final concentration of 1 μM as described earlier.[2] MV4-11/VENR cells were continually maintained in growth media with 1 μM of VEN. MV4-11/VENR cells were transduced with pFU-LUC2-EGFP lentiviral vector to stably express GFP and luciferase as described previously.[3] MV4-11 cells expressing YFP and luciferase were kindly provided by Kenichiro Doi.[4] U937 cells stably expressing the firefly

luciferase (LUC2) and tdTomato (Addgene plasmid #72486, RRID: Addgene_72486) were kindly gifted by Kazuhiro Oka. Other AML cell lines, including OCI-AML2, OCI-AML3, MOLM-13, MOLM-13-YFP-Luc, and U937, were obtained as mentioned in the acknowledgments.

Primary human AML cells were cultured in the serum-free medium StemSpan SFEM II (Stem Cell Technologies, Vancouver, BC, Canada) supplemented with cytokines (SCF, IL-3, FLT3-L, G-CSF, GM-CSF), StemRegenin1 (SR1), and 1X Penicillin-Streptomycin at 37°C in a humidified incubator with 5% CO_2 as described earlier.[5] AML patient samples were chosen based on the availability of adequate samples at the time of assay was performed.

Cell viability assays

The AML cell lines were seeded at 40,000 cells/well in 0.2 mL of media in a 96-well flat-bottom plate and treated with increasing concentrations of ROCK inhibitors (0.01-5 μM of DJ4, 5-125 μM of fasudil, 0.05-10 μM of GSK269962A-GSK) and VEN (0.01-20 μM) in combination. The cell viability was assessed by MTS assay after 24 h (VEN + DJ4 or fasudil) or 48 h (VEN + GSK) of treatment using MTS (CellTiter 96 Aqueous MTS reagent powder, #G1111, Promega) and phenazine methosulfate (PMS; #P9625, Sigma Aldrich) solution mix according to the manufacturer's protocol and as described earlier.[6,7] Absorbance measured at 490 nm by Molecular Devices SpectraMax i3x Multi-Mode Microplate Reader (RRID:SCR_026346) was presented as % viability relative to vehicle control (DMSO).

The viability of primary AML patient cells after treatment with GSK (0.125-1 μM) and VEN (0.06-2 μM) alone or in combination was measured using CellTiter-Glo luminescence assay (Promega, Cat# G755B). In brief, primary AML patient cells 24-48h post-thaw were seeded in serum-free SFEM media supplemented with cytokines at a density of 3 x 10^5 cells/mL in 96-well flat-bottom white plate to a final volume of 120 μL. After 48 h of treatment with increasing concentrations of GSK (0.125-1 μM) and VEN (0.06-2 μM) in combination, the cells were subjected to viability measurement using CellTiter-Glo reagent as per the manufacturer's protocol. Luminescence was measured using Molecular Devices SpectraMax i3x Multi-Mode Microplate Reader (RRID:SCR_026346) and represented as % viability relative to vehicle control. Viability data from drug combinations were used to generate dose-response matrices for synergy analysis.

Drug synergy analysis

Dose-response matrices containing % viabilities were used to compute synergy scores. The synergy between two drugs was analyzed using the SynergyFinder 2.0 web-application tool (https://synergyfinder.fimm.fi/, RRID:SCR_026127).[8] Bliss reference model was used to quantify the degree of interaction (synergy or antagonism) between drugs. Default parameters were used (Readout = Viability; Detect Outliers = Yes; Curve Fitting = LL4). Bliss scores (corrected for baseline) greater than 10, between 10 and −10, and below −10 are considered synergistic, additive, and antagonistic, respectively.

Clonogenic assay

Viable cryopreserved primary AML patient samples and cord blood mononuclear cells (CB-MNCs) were thawed at 37°C in IMDM medium containing 10% FBS. The colony-forming ability of primary AML patient cells in the presence of either GSK (0.25-2.5 μM) or VEN (0.5 μM) alone or in combination was tested by seeding cells at equal density in Human Methylcellulose Complete Media (R&D Systems, Minneapolis, MN, USA) in a 12-well cell culture plate in triplicate and incubating for 10-14 days, as reported earlier.[5] Colonies (>20 cells/colony) were counted under an Olympus CKX31 inverted light microscope (Olympus Corporation, Center Valley, PA, USA) and imaged using a 4x objective. The data was represented as % colonies relative to the solvent (DMSO) control. Samples were chosen based on the availability of adequate samples at the time of assay was performed.

Measurement of apoptosis, ROS, and mitochondrial membrane potential

The AML cells were seeded at a density of 4 x 10^5 cells/ml in a 12-well plate and left untreated or treated with vehicle (DMSO), GSK, VEN alone, or in combination at the indicated concentration. After 48 h of treatment, Annexin V positivity, Caspase-3/7 activity, reactive oxygen species (ROS) levels, and mitochondrial membrane potential ($\Delta\Psi_m$) were assessed using Muse Annexin V & Dead Cell Kit (Cytek, Cat# MCH100105), Muse Caspase-3/7 Kit (Cat# MCH100108), Muse Oxidative Stress Kit (Cat# MCH100111), and Muse MitoPotential Kit (Cytek, #MCH100110) respectively, following the manufacturer's instructions.[5,7] For each sample, at least 2000 events were acquired using Muse Cell Analyzer (RRID:SCR_020252) and represented as a percentage of positive cells.

Assessment of mitochondrial membrane potential ($\Delta\Psi_m$) in whole intact cells

MV4-11 (naïve and VENR) cells were seeded at 0.4 x 10^6 cells/ml in IMDM growth media and treated with vehicle, indicated doses of either GSK, VEN, or the GSK+VEN combination. After 15 and 24 h of treatment, 3 ml of cells from each treatment were divided into unstained, vehicle, and FCCP (carbonyl cyanide p-trifluoromethoxyphenylhydrazone) tubes with 1 ml each. After this, cells were treated with either vehicle (DMSO) or FCCP (5 μM; Sigma, #C2920) for 15 min at 37°C. The cells were stained with 20 nM of Tetramethylrhodamine methyl ester (TMRM; Thermo Fisher Scientific, #T668) and incubated for 30 min at 37°C. Thereafter, 4′,6-diamidino- 2- phenylindole (DAPI; Thermo Fisher Scientific, #62248) was added at 1 μg/ml. Samples were then analyzed using BD LSRFortessa flow cytometer (BD Bioscience) at the core facility of Pennsylvania State University. Data was analyzed by excluding nonviable cells (DAPI positive), and the median fluorescence intensity of TMRM normalized to mitochondrial uncoupler FCCP (negative control) was expressed as % of the vehicle group.[2] FlowJo software version 10.0.7 (RRID:SCR_008520) was used for data analysis.

Mitochondrial respiratory profiling in intact and permeabilized cells

High-resolution respirometry measurements were performed at 37°C using the Oroboros Oxgraph-2k (O2k; Oroboros Instruments, Innsbruck, Austria) in a 0.5 - 1 mL reaction volume and normalized to viable (trypan blue exclusions) cell count as described earlier.[2] For respiratory flux (OXPHOS) measurements in intact cells, MV4-11/VENR cells were resuspended in Intact Cell Respiratory Media (17.7 g/L Iscove's Modified Dulbecco's Medium (IMDM), 20 mM HEPES, 1% Penicillin/Streptomycin, 10% FBS, pH 7.4) after overnight treatment either with vehicle or 400 nM GSK. After basal respiration was established, the maximal rate of respiration was induced by FCCP titration (0.5–5 mM). For permeabilized cell measurements, MV4-11/VENR cells were resuspended in Respiratory Buffer supplemented with creatine (105 mM MES potassium salt, 30 mM KCl, 8 mM NaCl, 1 mM EGTA, 10 mM KH_2PO_4, 5 mM $MgCl_2$, 0.25% BSA, 5 mM creatine monohydrate, pH 7.2) after overnight treatment with either vehicle or 400 nM GSK. Cells were permeabilized using 0.02 mg/mL of digitonin, and then the respiratory capacity of different complexes was measured by energizing the mitochondria with inhibitors and carbon substrates as follows: pyruvate, malate, and ADP (Complex I; 5/1/2 mM), rotenone (Rot, 0.5 mM), succinate (Complex II; 5 mM), malate (Malo; 10 mM), and N,N,N',N'-tetramethyl-p-phenylenediamine (TMPD)/ascorbate (Asc) (Complex IV; 0.05/2 mM).

Western blotting

The AML cell lines (MV4-11 and MV4-11/VENR) were seeded at a density of 4 x 10^5 cells/ml in T25 or T75 cell culture flasks and left untreated or treated with DMSO (vehicle), GSK, VEN alone, or in combination at the indicated doses and time. After the incubation period, the cells were pelleted, and whole cell lysates were prepared in RIPA buffer (Sigma; #R0278) supplemented with 1X Halt Protease and Phosphatase Inhibitor Cocktail (ThermoFisher Scientific; #78442) prior to being subjected to immunoblotting analysis as described earlier.[6] Briefly, equal amounts of protein after BCA assay quantification were subjected to gel electrophoresis using NuPAGE 4–12% Bis-Tris gel (Life Technologies, Carlsbad, CA, USA). Proteins were transferred to PVDF membrane prior to probing with the following antibodies: ROCK1 (BD Biosciences; #611136, RRID:AB_398447), ROCK2 (BD Biosciences; #610623, RRID:AB_397955), Cofilin (Cell Signaling; #5175S, RRID:AB_10622000), phospho-Cofilin (Cell Signaling; #3313S, RRID:AB_2080597), Drp1 (Cell Signaling; #5391, RRID:AB_11178938), phospho-Drp1 (Cell Signaling; #4494, RRID:AB_11178659), phospho-PTEN (Cell signaling; #9549S, RRID:AB_659891), NOXA (Santa Cruz Biotechnology; #sc-56169, RRID:AB_784877), Bcl-2 (Cell signaling; # 3498S, RRID:AB_1903907), phospho-Bcl-2 (Cell signaling; #2827S, RRID:AB_659950), Mcl1 (Cell signaling; #5453, RRID:AB_10694494), Bcl-xL (Cell signaling; #2764S, RRID:AB_2228008), Bak (Cell signaling; #12105S, RRID:AB_2716685), PARP (Cell signaling; #9542S, RRID:AB_2160739), Caspase-3 (Cell signaling; # 9662S, RRID:AB_331439), β-Actin (Santa Cruz Biotechnology; #sc-47778, RRID:AB_626632), and GAPDH (Santa Cruz Biotechnology; #sc-32233, RRID:AB_627679). The goat anti-rabbit IgG–horseradish peroxidase (HRP) conjugates (#7074S, RRID: AB_2099233) and the horse anti-mouse IgG-HRP conjugates (#7076S, RRID:AB_330924) were purchased from Cell Signaling Technology. The chemiluminescent signals were captured using the Bio-Rad ChemiDoc MP imaging system (Bio-Rad Laboratories, Hercules, CA, USA) and quantified via the ImageJ software (https://imagej.net/ij/, RRID:SCR_003070). The band densities were relative to GAPDH levels and normalized to an untreated reference that was set to 1.

In vivo mice efficacy and safety studies

All animal experimental protocols were approved by the Institutional Animal Care and Use Committee (IACUC), and the mice were procured either from Jackson Lab, Charles River Laboratory, or bred at Penn State University.

Cell line-derived xenografts (CDX): Cell line-derived xenografts were established to test *in vivo* efficacy of GSK and VEN combination as described previously.[5-7] Briefly, luciferase-expressing AML cell lines (2.5 x 10^6 of

MV4-11-YFP-Luc, 2 x 10^6 of MV4-11/VENR-EGFP-Luc, 0.5 x 10^6 of MOLM-13-YFP-Luc, and 1 x 10^4 of U937-Luc- tdTomato) were intravenously injected into 6-9-week-old NOD Cg-Rag1tm1Mom Il2rgtm1Wjl Tg(CMV-IL3,CSF2,KITLG)1Eav/J (NRG-S) mice (RRID:IMSR_JAX:024099) and randomized to experimental groups based on bioluminescence imaging (BLI) signals and body weight. All female or male mice were used per study, and the mice were treated with either vehicle, GSK (10mg/kg, i.p., Mon-Fri), VEN (50-100 mg/kg, p.o., Mon-Fri), or both GSK and VEN for 2-3 weeks as indicated. VEN was formulated in 10% ethanol/30% polyethylene glycol 400 (PEG400)/60% phosal 50 propylene glycol (PG) (v/v/v),[9] and GSK was dissolved in 20% PEG300/0.25% Tween-80/79.75% water,[10] as reported earlier. Dosing regimens were selected based on published pharmacokinetic data for VEN and GSK269962A. VEN has been reported to exhibit oral half-lives of approximately 4–6 h in mice and 6–10 h in rats, with systemic exposures sufficient to support once-daily dosing.[11,12] In contrast, GSK269962A demonstrates a shorter reported half-life of ~1–3 h with moderate oral bioavailability in rodents,[13] supporting the dosing schedules used in this study. The mice were regularly imaged once a week or as indicated using the Perkin Elmer IVIS Lumina LT Series III imaging system (RRID:SCR_018621) after 7 min of D-luciferin (Gold Biotechnology, St. Louis, MO) intraperitoneal injection (150 mg/kg). The leukemia burden was quantified using Living Image software (Perkin Elmer) and represented as average radiance (p/s/cm²/sr). After the treatment period, peripheral blood samples were collected through submandibular puncture and subjected to flow cytometry analysis. The mice were either monitored for overall survival and subjected to Kaplan–Meier analysis or bone marrow (BM) cells were harvested to evaluate leukemic burden by flow cytometry.

Patient-derived xenograft (PDX): PDX model was first established by injecting AML Pt. 1265 primary cells (24h post-transduction with pLV-EF1a-LUC2-T2A-EGFP lentiviral vector) into NRG-S mice as described earlier with modifications.[14,15] Briefly, the primary AML cells were mixed with anti-human CD3 (OKT-3) monoclonal antibody (Bio X Cell, #BE0001-2, RRID: AB_1107632; for T-cell depletion *in vivo*) prior to injection into NRG-S mice irradiated with 200 rad of γ-rays a day prior. The BM cells collected from PDX mice were sorted for GFP positivity, cultured in serum-free growth medium, and injected into secondary recipient mice for enrichment of labeled patient cells. The BM cells collected from secondary PDX mice were transplanted into NRG-S mice for establishing the bioluminescent PDX model. After 13 days of transplant, the mice were randomized into four experimental groups (control, GSK, VEN, and GSK+VEN) based on BLI signals (n=5-7). The mice were treated

with either GSK (30 mg/kg, p.o.), VEN (50 mg/kg, p.o.), or the combination of GSK and VEN once daily for 6 days/week for a total of 3 weeks. After the end of the treatment, the leukemia burden was periodically monitored by IVIS imaging. On day 148 (21 weeks) post-transplant, the bone marrow cells were collected from all the experimental groups and checked for human AML (donor) chimerism by flow cytometry.

Mouse safety study: The short (2 weeks) and long-term subchronic (4 weeks) safety and toxicity of the GSK269962A and VEN combination were evaluated by treating 6- to 8-week-old female Swiss Webster mice (Charles River Laboratory, RRID:IMSR_CRL:024) with either vehicle, GSK (30 mg/kg, p.o.), VEN (50 or 100 mg/kg, p.o.), or the GSK+VEN combination once daily, six days per week (Mon-Sat), for two or four weeks. After 2- or 4-weeks of treatment, blood samples were collected from mice through cardiac puncture to run a complete blood count (CBC) by Hemavet 950FS analyzer (Drew Scientific, Plantation, FL, USA) and clinical chemistry for assessing the renal and liver functions (VRL Diagnostics, Gaithersburg, MD, USA).

Flow cytometry

The peripheral blood or bone marrow cells collected from CDX or PDX mice were analyzed for the presence of human AML cells (CD45 positive) by flow cytometry.[6,16] Briefly, whole blood or bone marrow cells were treated with BD Pharm Lyse Lysing Buffer (BD Biosciences, #555899) to lyse red blood cells followed by washing with fluorescence-activated cell sorting (FACS) buffer (Dulbecco's phosphate buffered saline with 2% FBS). Cells were incubated with cocktail of Human BD Fc Block (BD Biosciences, #564220, RRID:AB_2869554) and Mouse BD Fc Block (BD Biosciences, #553141, RRID:AB_394656) for 10 minutes at room temperature to prevent nonspecific antibody binding and then stained with following antibodies: human CD45-APC/Cy7 (BioLegend, #304014, RRID:AB_314402) or human CD45-PE (BioLegend, #368510, RRID:AB_2566370), human CD34-FITC (BD Biosciences, #555821, RRID:AB_396150), mouse CD45-BV650 (BD Biosciences, #563410, RRID:AB_2738189) cocktail for 20 minutes on ice in the dark, followed by washing with FACS buffer. Finally, the cells were suspended in FACS buffer with viability dye 7-AAD (BioLegend, #420404) and analyzed by BD LSR Fortessa Flow Cytometer (BD Bioscience) and processed using FlowJo version 10.0 (RRID:SCR_008520). Engraftment of human cells (chimerism) in peripheral blood or bone marrow was detected using the appropriate fluorochrome filters and reported as the percentage of positive cells.

Supplementary Figures:

A

S.No.	Target Gene	Day 16 delta CS	Day 16 p value
1	RHOA	-3.657	0.0505
2	ROCK1	-0.410	0.7850
3	ROCK2	-1.488	0.3017
4	MYL2	-2.364	0.0347
5	MYL9	-2.388	0.1719
6	PPP1CA	-1.243	0.1569
7	PPP1CB	-0.645	0.3618
8	PPP1CC	-1.450	0.0195
9	PPP1R12A	-2.224	0.0116
10	PPP1R12B	-1.847	0.1616
11	PIP5K1A	-3.130	0.0058
12	PIP5K1C	-2.211	0.1457
13	RAC1	-0.314	0.8853
14	RAC2	-2.358	0.0185
15	RAC3	-1.410	0.1617
16	PAK1	-2.001	0.0915
17	PAK2	-0.978	0.3542
18	PAK3	-2.460	0.0030
19	PAK4	-2.228	0.0233

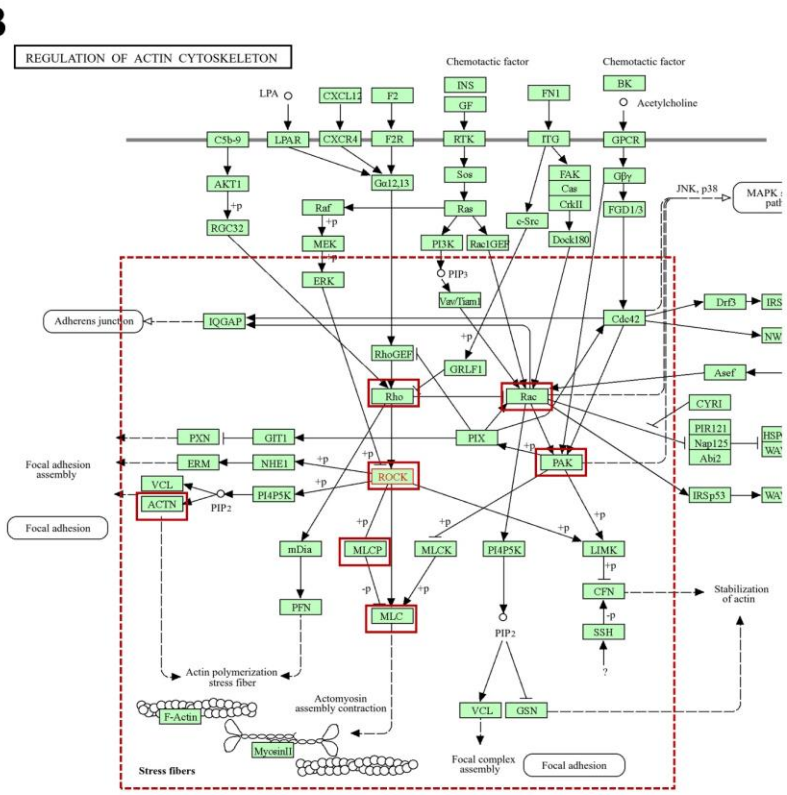

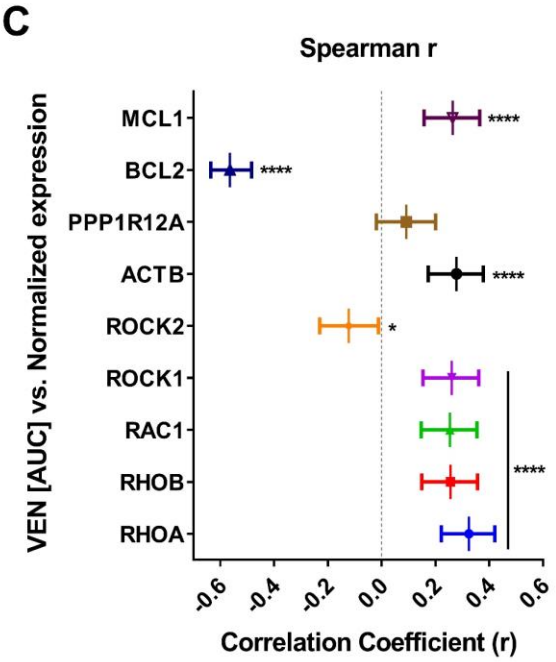

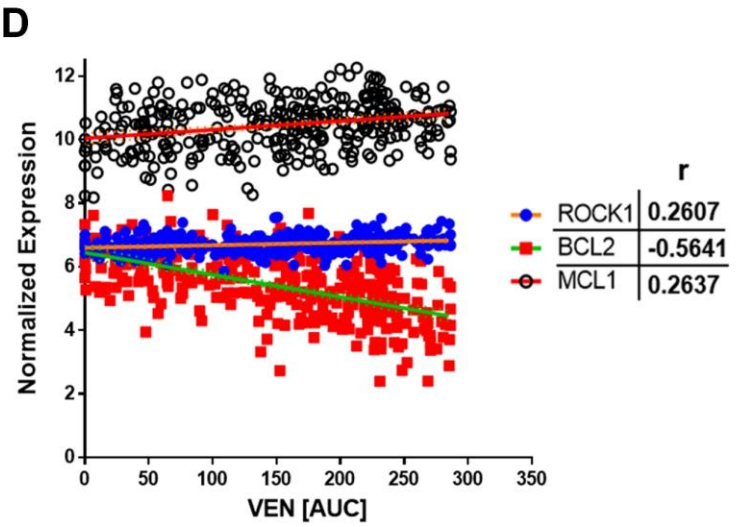

Supplementary Figure 1: The Rho/ROCK pathway cooperates with venetoclax activity in AML cells. A) Rho/ROCK pathway genes are negatively enriched (genes whose loss synergizes with venetoclax) in a CRISPR/Cas9 loss-of-function screen in MOLM-13 cells after 16 days of VEN treatment. The delta CRISPR scores (CS) and the corresponding p-values for the selected genes were adopted from Chen X et al. [17]. B) KEGG pathway map (https://www.kegg.jp/entry/map04810) for 'Regulation of actin cytoskeleton' highlights the Rho/ROCK pathway genes that are negatively enriched in the CRISPR loss-of-function screen after VEN treatment. C & D) Spearman correlation analysis comparing venetoclax area under the curve (AUC) against normalized mRNA expression of BCL-2, MCL1, and Rho/ROCK pathway genes. The correlation coefficient (r) for different genes (C) and a representative correlation plot for BCL-2, MCL1 and ROCK1 genes (D) was shown. We used MCL1 and BCL-2 genes as controls, and accordingly, their expression levels resulted in a positive and negative correlation with VEN AUC, respectively. Data (n=332) were obtained from BeatAML2.0 (http://www.vizome.org/aml2/). *p<0.05 and ****p<0.0001 (two-tailed) indicate statistical significance.

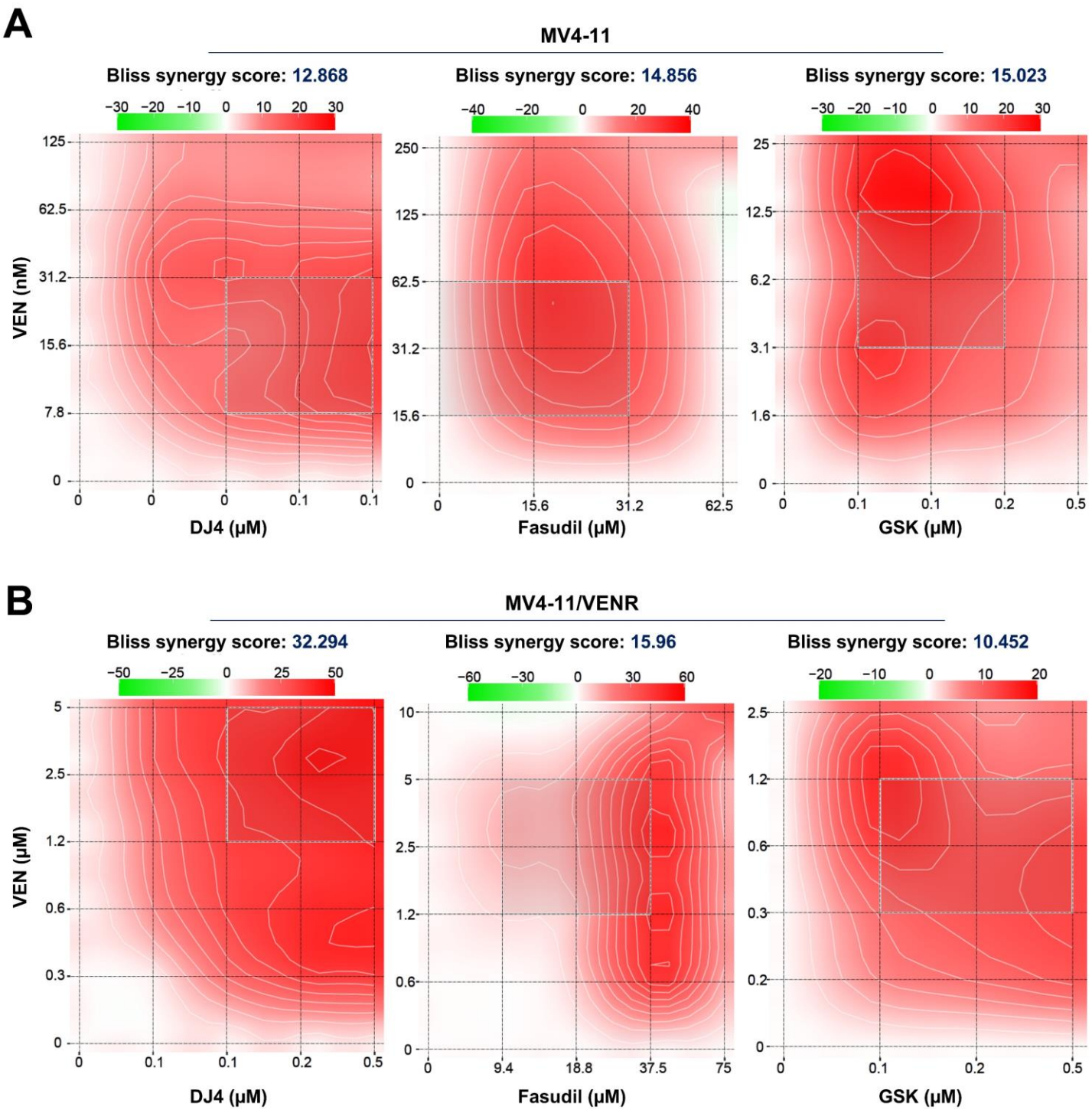

Supplementary Figure 2: ROCK inhibitors exhibit synergistic cytotoxicity with venetoclax combination in AML cell lines *in vitro*. A & B) Heatmap showing the Bliss synergy score in MV4-11 (A) and MV4-11/VENR (B) cells after ROCKi and VEN combination treatment for 24h (DJ4, Fasudil) and 48h (GSK269962A-GSK). Bliss scores greater than 10 were considered synergistic. Representative plots from at least three independent experiments are presented.

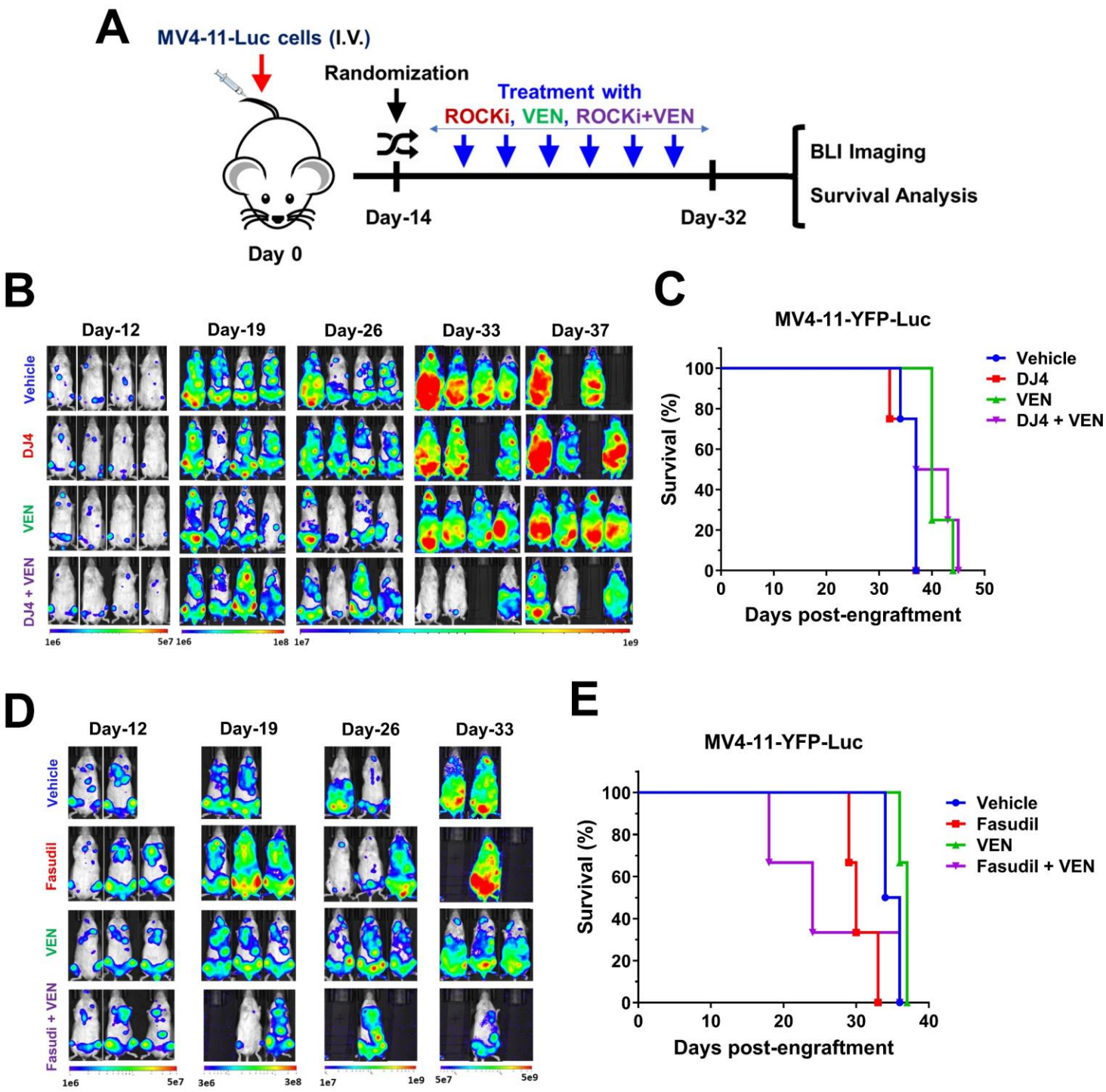

Supplementary Figure 3: Combination of VEN with ROCKi (Fasudil and DJ4) exhibit modest efficacy in the MV4-11 CDX mouse model. A) Schematic depicting the randomization of NRG-S (n=2-4) mice into four experimental groups (vehicle, ROCKi-DJ4 or fasudil, VEN, and ROCKi+VEN combo) based on BLI signals after 12 days of post-injection of MV4-11-YFP-Luc cells intravenously. Fasudil (25mg/kg; i.p.; M-F) or DJ4 (10mg/kg; i.p.; M-F) combined with VEN (100mg/kg; p.o.; M-F) for mice treatments. B & D) The MV4-11 CDX mice were monitored regularly by IVIS imaging at indicated days. C & E) Kaplan-Meier survival analysis of MV4-11 CDX mice after treatment with ROCKi (DJ4 or Fasudil), VEN, and the ROCKi+VEN combination. The Gehan-Breslow-Wilcoxon test indicated that the overall survival of mice was not statistically different for treatment groups compared to vehicle control.

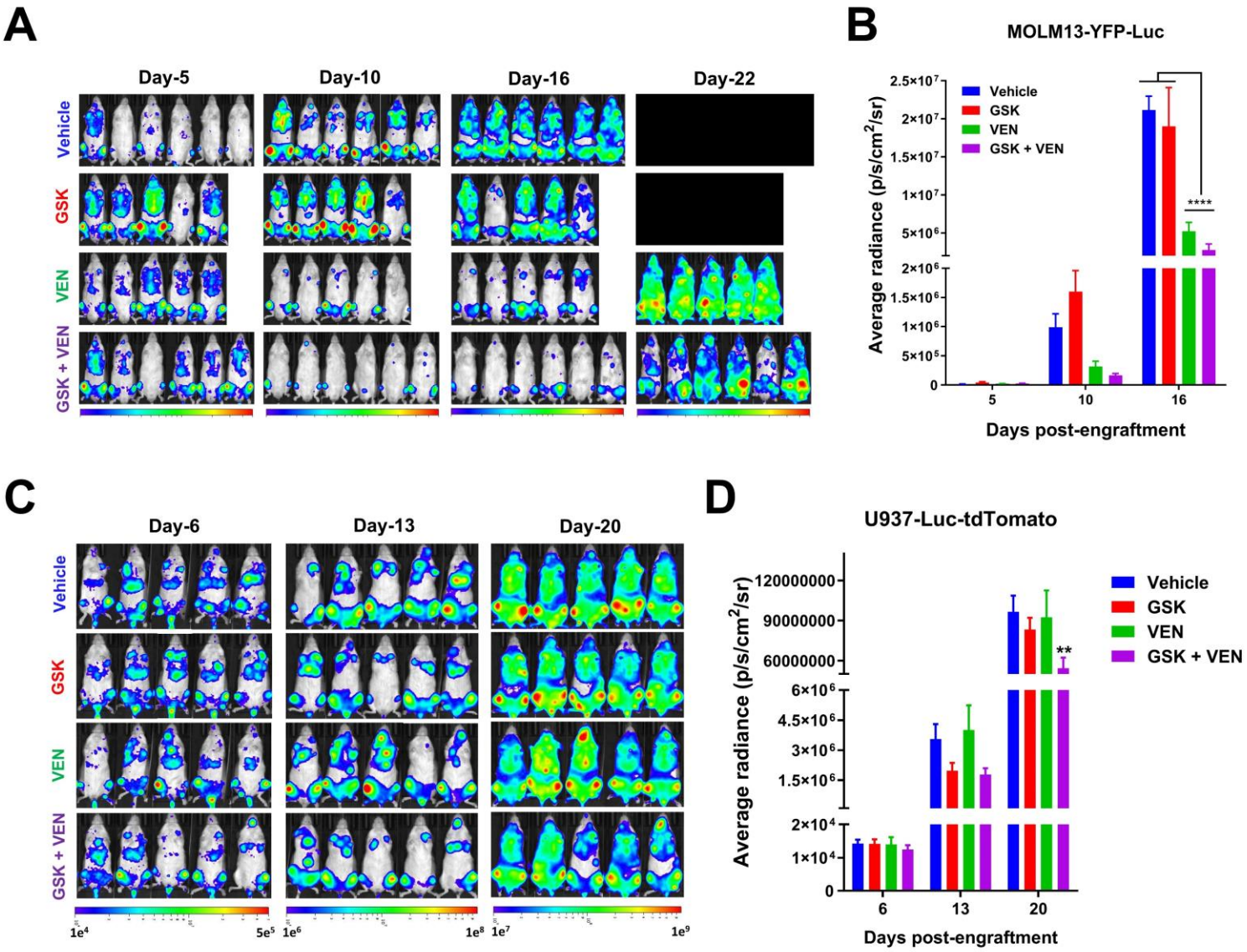

Supplementary Figure 4: GSK and VEN combination synergistically decrease leukemia burden in AML cell line xenograft models. A & C) Bioluminescence imaging of MOLM13-YFP-Luc (A) and U937-Luc-tdTomato (C) CDX mice at indicated days, as described in Figure 2. The NRG-S mice (n=5-6) were intravenously injected with AML cells (MOLM13-YFP-Luc, and U937-Luc-tdTomato) and randomized into experimental groups (Vehicle, GSK, VEN, and GSK+VEN). B & D) The leukemia burden in the MOLM13-YFP-Luc (B) and U937-Luc-tdTomato (D) CDX mice was quantified in the terms of BLI signals and presented as average radiance (p/s/cm^2/sr). **p<0.01, ****p<0.0001 by 2-way ANOVA (Tukey's multiple comparisons test) compared to vehicle control.

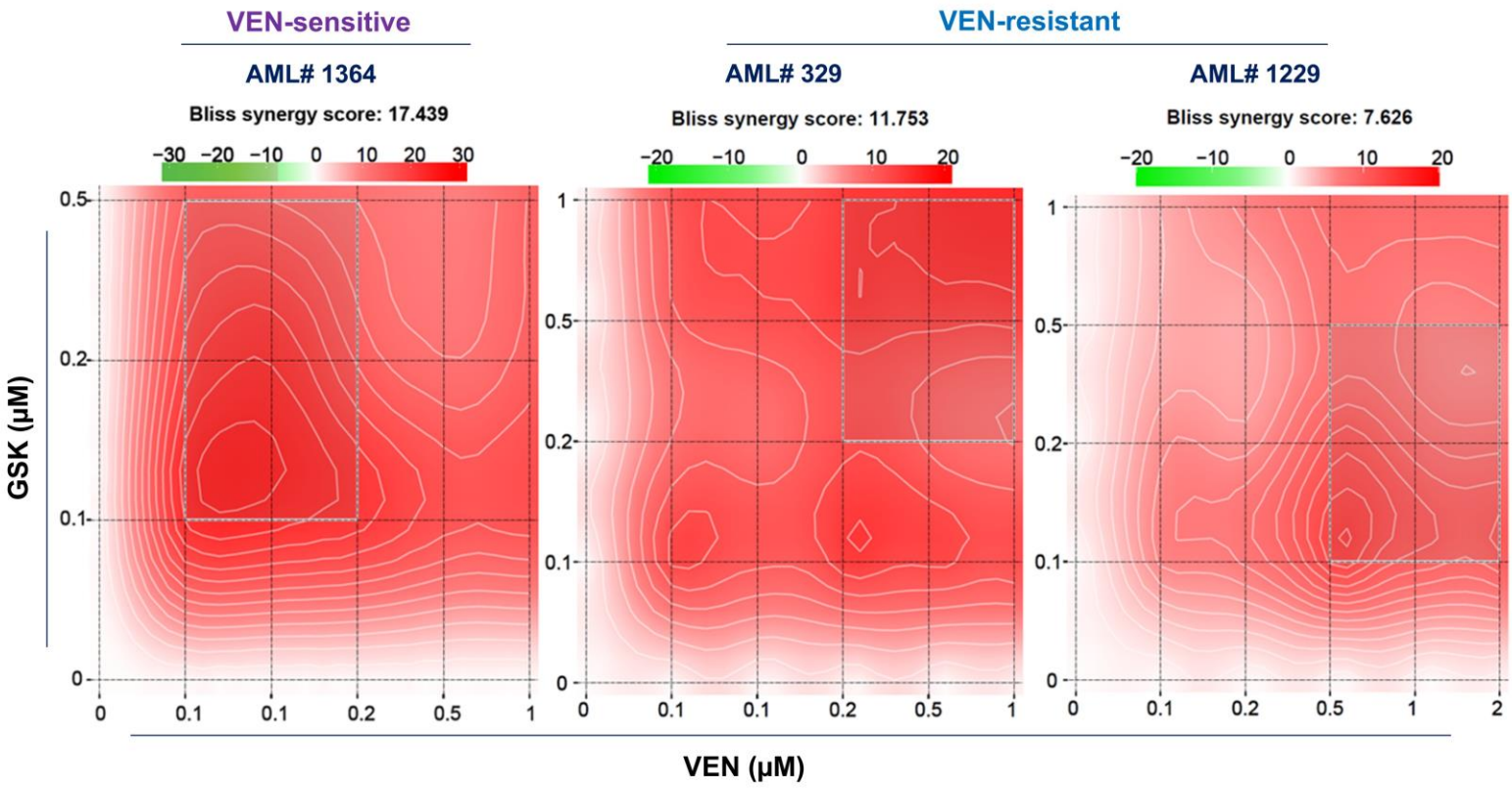

Supplementary Figure 5: ROCK inhibitors exhibit synergistic cytotoxicity with venetoclax combination in primary AML patient cells *ex vivo*. Heatmap showing the Bliss synergy score for primary AML patient cells (VEN-sensitive and VEN-resistant) after GSK and VEN combination treatment. The cell viability of patient cells was measured by the CellTiter-Glo assay. Bliss scores greater than 10 indicate 'synergy,' and 0-10 indicate 'additive' activity.

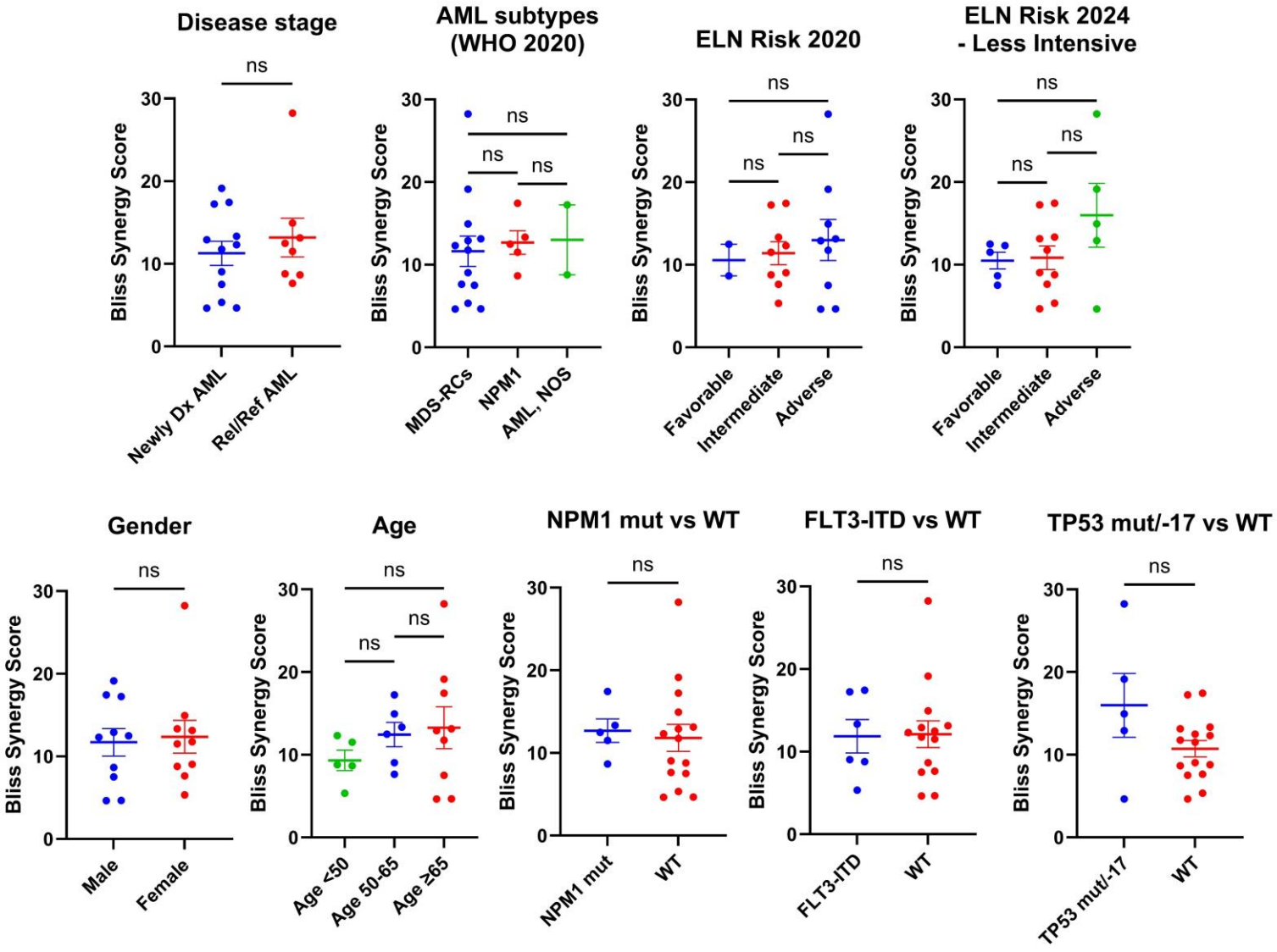

Supplementary Figure 6: Subgroup analysis of Bliss synergy scores for primary AML patient cells after treatment with GSK and VEN combination. Comparative analyses of the Bliss synergy scores after 48h of GSK+VEN combination treatment among subgroups of primary AML patient cells (n=20) disease characteristics, as defined according to baseline demographic and disease characteristics. Data are presented as mean ± SEM and *p<0.05 is considered statistically significant when analyzed by either unpaired t-test (two groups) or one-way ANOVA (three groups). 'ns' denotes 'not significant'.

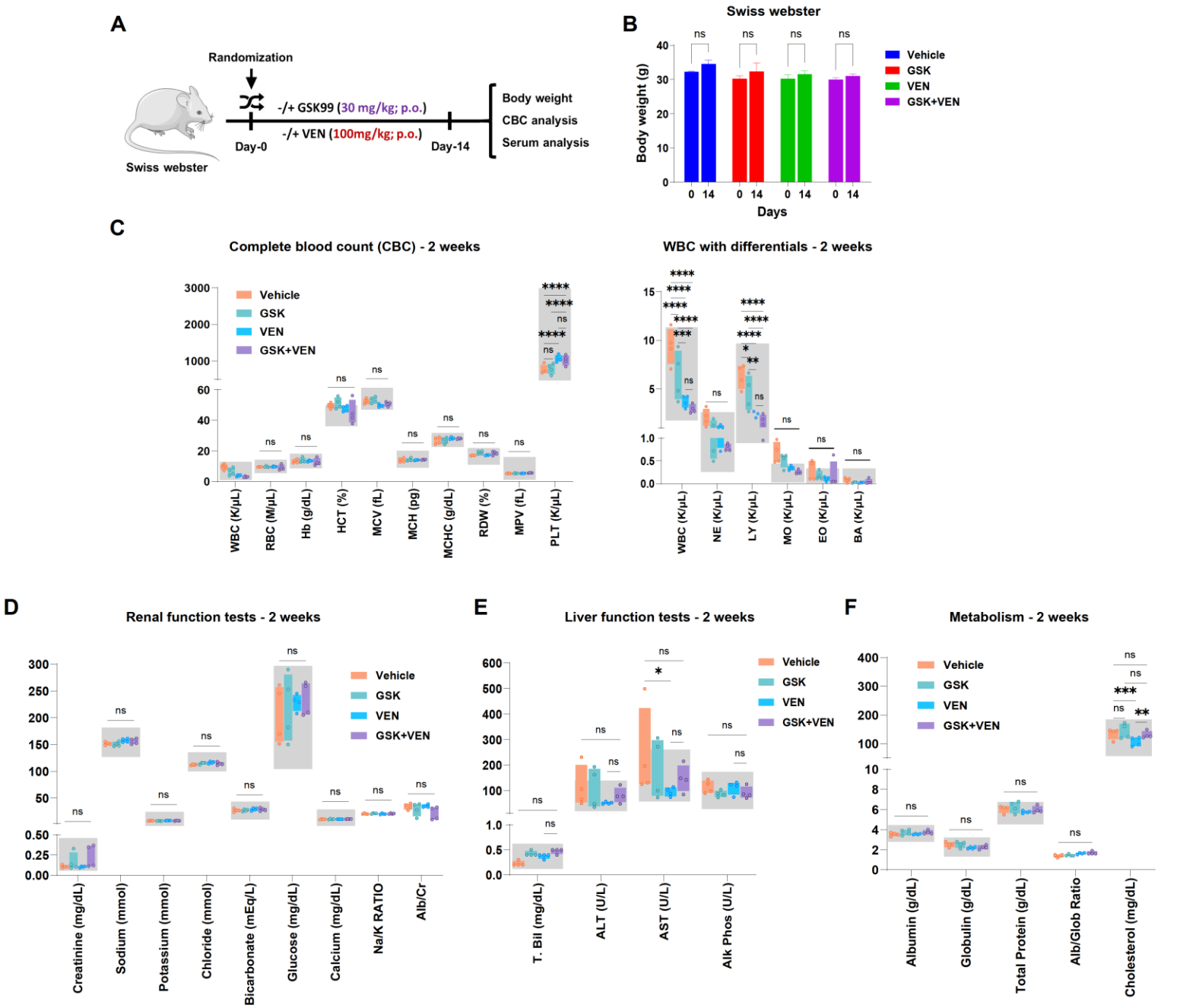

Supplementary Figure 7: Short-term (2-weeks) safety profile of GSK alone and in combination with VEN. A) Schematic depicting the randomization of Swiss Webster mice (n=4) into four experimental groups (vehicle, GSK, VEN, and GSK+VEN combo). B) Body weight (g) of experimental Swiss Webster mice before and after 2-weeks of treatment with either vehicle, GSK (30 mg/kg, p.o., Mon-Sat), VEN (100 mg/kg, p.o., Mon-Sat), or GSK+VEN combination. C) CBC analysis of normal Swiss Webster mice after 2-weeks of treatment. D-F) Serum collected from Swiss Webster mice after 2-weeks of treatment and subjected to clinical chemistry. The shaded area represents the normal ranges for each parameter. Data are presented as mean ± SD (n=4), and *p<0.05, **p<0.01, ***p<0.001, and ****p<0.0001 were considered statistically significant compared to vehicle when analyzed by 2-way ANOVA (Tukey's multiple comparisons test). 'ns' denotes 'not significant'.

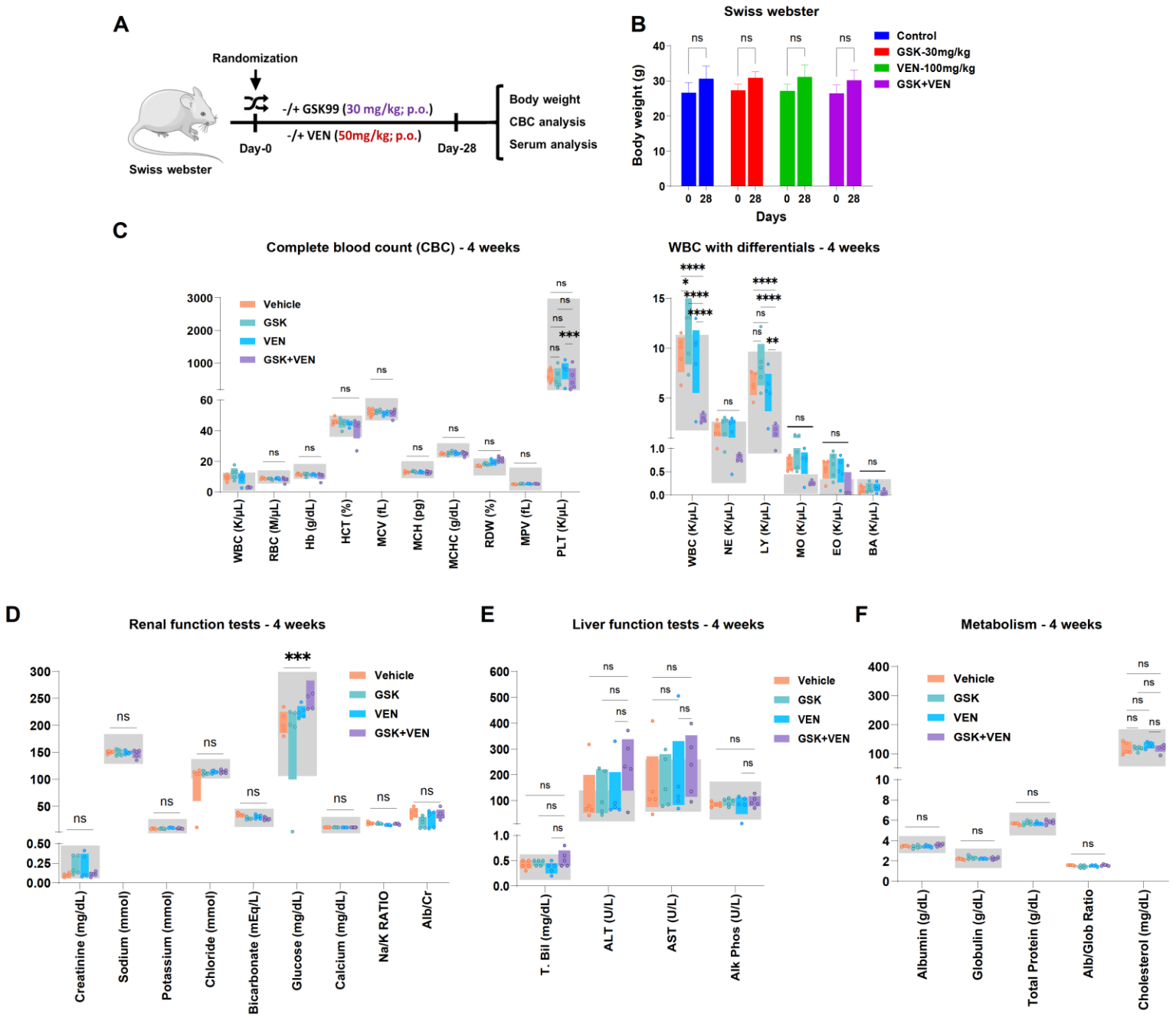

Supplementary Figure 8: Long-term (4-weeks) safety profile of GSK alone and in combination with VEN. A) Schematic depicting the randomization of Swiss Webster mice (n=5) into four experimental groups (vehicle, GSK, VEN, and GSK+VEN combo). B) Body weight (g) of experimental Swiss Webster mice before and after 4-weeks of treatment with either vehicle, GSK (30 mg/kg, p.o., Mon-Sat), VEN (50 mg/kg, p.o., Mon-Sat), or GSK+VEN combination. C) CBC analysis of normal Swiss Webster mice after 4-weeks of treatment. D-F) Serum collected from Swiss Webster mice after 4-weeks of treatment and subjected to clinical chemistry. The shaded area represents the normal ranges for each parameter. Data are presented as mean ± SD (n=5), and *p<0.05, **p<0.01, ***p<0.001, and ****p<0.0001 were considered statistically significant compared to vehicle when analyzed by 2-way ANOVA (Tukey's multiple comparisons test). 'ns' denotes 'not significant'.

Supplementary Tables

Supplementary Table 1: IC_{50} values for AML cell lines after 24h (VEN, DJ4, Fasudil) and 48h (GSK) of treatment assessed by MTS assay.

AML cell line	IC_{50} Concentration (μM)			
	VEN	DJ4	Fasudil	GSK
MV4-11	0.036	0.145	29.68	0.143
MV4-11/VENR	>5	0.257	42.25	0.387
MOLM-13	0.02	0.307	66.23	3.08
HL-60	0.033	1.097	53.97	>5
OCI-AML2	0.007	1.075	26.98	1.07
OCI-AML3	7.63	1.14	47.62	1.19
KG-1	>10	1.548	32.43	1.89
U937	>10	1.89	116	>5

Supplementary Table 2: Serum biochemistry analysis of renal, liver, and metabolic parameters in mice treated with vehicle, GSK, VEN, or the GSK+VEN combination for 2 or 4 weeks.

Renal function	Normal ranges	2 weeks				4 weeks			
		Vehicle	GSK	VEN	GSK+VEN	Vehicle	GSK	VEN	GSK+VEN
Creatinine (mg/dL)	0.12 - 0.43	0.11 ± 0.02	0.16 ± 0.11	0.1 ± 0.01	0.24 ± 0.14	0.1 ± 0.02	0.22 ± 0.12	0.2 ± 0.16	0.11 ± 0.03
Sodium (mmol)	124.81 - 160.31	151.48 ± 2.87	150.35 ± 4.37	157.55 ± 3.63	155.93 ± 5.29	150.16 ± 2.61	148.86 ± 5.97	149.62 ± 3.17	147.38 ± 7.69
Potassium (mmol)	2.17 - 8.18	7.44 ± 0.33	7.22 ± 0.17	7.85 ± 0.29	7.52 ± 0.29	8.26 ± 1.01	8.44 ± 0.83	10.03 ± 0.55	8.92 ± 0.9
Chloride (mmol)	99.96 - 121.75	112.1 ± 1.21	114.88 ± 1.92	116.23 ± 2.03	114.03 ± 2.88	91.98 ± 45.53	111.36 ± 3.11	113.48 ± 2.61	113.98 ± 3.41
Bicarbonate (mEq/L)	5.86 - 30.91	26.9 ± 3	26.95 ± 2	28.9 ± 2.59	28.38 ± 2.95	34.22 ± 2.76	27.44 ± 2.25	30.48 ± 3.94	26.64 ± 2.84
Calcium (mg/dL)	8.28 - 12.27	10.23 ± 0.5	10.45 ± 0.73	10.38 ± 0.13	10.65 ± 0.37	10.98 ± 0.39	10.84 ± 0.29	10.68 ± 0.15	10.88 ± 0.18
Na/K RATIO		20.5 ± 1	21 ± 0.82	20.25 ± 1.26	20.75 ± 0.96	18.6 ± 2.41	17.8 ± 1.3	15.2 ± 0.84	17 ± 1.22
Alb/Cr		34.23 ± 5.65	29.15 ± 12.43	34.84 ± 2.91	21.18 ± 12.28	37.8 ± 9.01	19.83 ± 10.41	26.64 ± 15.84	34.68 ± 9.61

Liver function	Normal ranges	2 weeks				4 weeks			
		Vehicle	GSK	VEN	GSK+VEN	Vehicle	GSK	VEN	GSK+VEN
T. Bil (mg/dL)	0.17 - 0.53	0.23 ± 0.05	0.43 ± 0.05	0.38 ± 0.05	0.48 ± 0.05	0.42 ± 0.08	0.46 ± 0.05	0.36 ± 0.11	0.54 ± 0.17
Alk Phos (U/L)	62-209	114.5 ± 25	86.75 ± 12.5	112 ± 25.97	90.75 ± 23.82	114.2 ± 114.7	127.8 ± 86.57	125.2 ± 114.98	236.8 ± 118.1
ALT (U/L)	28-132	113.25 ± 81.96	109.5 ± 79.71	51.25 ± 4.65	81 ± 30.56	160.2 ± 142.69	173.2 ± 101.22	189 ± 179.86	235.4 ± 123.71
AST (U/L)	59-247	237.75 ± 177.11	187.75 ± 118.25	94.75 ± 17.46	147.5 ± 53.21	85.4 ± 9.5	94.8 ± 14.6	81.2 ± 41.52	96.6 ± 21.52

Metabolism	Normal ranges	2 weeks				4 weeks			
		Vehicle	GSK	VEN	GSK+VEN	Vehicle	GSK	VEN	GSK+VEN
Glucose (mg/dL)	106.74 - 353.74	206.75 ± 54.36	218.75 ± 64.1	228.75 ± 15.41	235 ± 31.95	204 ± 21.3	169.8 ± 94.09	224.6 ± 11.84	256.2 ± 31.28
Total Protein (g/dL)	4.48 - 6.32	6.05 ± 0.37	6.25 ± 0.58	5.75 ± 0.13	5.98 ± 0.36	5.66 ± 0.09	5.74 ± 0.21	5.68 ± 0.13	5.84 ± 0.24
Cholesterol (mg/dL)	52.62 - 167.47	135 ± 19.37	143.5 ± 26.49	106.75 ± 15.59	130.25 ± 12.69	1.58 ± 0.04	1.46 ± 0.15	1.52 ± 0.08	1.58 ± 0.08
Albumin (g/dL)	3.60 1.92 - 4.11	3.53 ± 0.17	3.73 ± 0.28	3.55 ± 0.06	3.73 ± 0.19	3.46 ± 0.05	3.4 ± 0.16	3.44 ± 0.11	3.6 ± 0.14
Globulin (g/dL)	0.92 - 3.64	2.53 ± 0.25	2.53 ± 0.31	2.2 ± 0.12	2.25 ± 0.21	2.2 ± 0.07	2.34 ± 0.17	2.24 ± 0.05	2.26 ± 0.13
Alb/Glob Ratio		1.4 ± 0.14	1.45 ± 0.1	1.63 ± 0.1	1.68 ± 0.15	117.8 ± 21.16	118 ± 8.72	128.4 ± 10.83	118 ± 14.09

All values are presented as mean ± SD (n=4-5) with corresponding normal reference ranges for mice.

Supplementary Table 3: Complete blood count and leukocyte differentials in mice treated with vehicle, GSK, VEN, or the GSK+VEN combination for 2 or 4 weeks.

CBC with differentials	Normal ranges	2 weeks				4 weeks			
		Vehicle	GSK	VEN	GSK+VEN	Vehicle	GSK	VEN	GSK+VEN
RBC (M/µL)	6.36-9.42	9.47 ± 0.11	9.62 ± 0.47	9.6 ± 0.34	8.9 ± 1.8	8.86 ± 0.52	8.52 ± 0.58	8.73 ± 0.51	8.05 ± 1.63
Hb (g/dL)	11-15.1	13.2 ± 1.23	13.68 ± 1.64	13.38 ± 0.54	12.6 ± 2.38	11.48 ± 0.61	11.42 ± 1.15	11.28 ± 0.54	10.36 ± 2.4
HCT (%)	35.1-45.4	49.48 ± 1.85	51.08 ± 3.8	47.53 ± 2.04	44.98 ± 7.94	46.04 ± 2.21	44.88 ± 3.28	44.7 ± 1.7	41.16 ± 8.08
MCV (fL)	45.4-60.3	52.25 ± 1.73	53.13 ± 2.12	49.5 ± 0.98	50.7 ± 1.5	52.04 ± 2.46	52.66 ± 1.08	51.3 ± 1.28	51.26 ± 2.71
MCH (pg)	14.1-19.3	13.93 ± 1.4	14.18 ± 0.99	13.95 ± 0.26	14.18 ± 0.26	12.96 ± 0.71	13.34 ± 0.52	12.94 ± 0.55	12.8 ± 0.98
MCHC (g/dL)	30.2-34.2	26.68 ± 2.37	26.73 ± 2.05	28.15 ± 0.76	27.98 ± 0.43	24.94 ± 0.48	25.42 ± 1.24	25.24 ± 0.82	24.98 ± 1.38
RDW (%)	12.4-27	17.05 ± 0.13	18.83 ± 1.13	17.25 ± 0.26	18.4 ± 1.29	17 ± 0.33	18.26 ± 0.67	19.56 ± 1.58	21.3 ± 1.79
MPV (fL)	5.0-20.2	5.18 ± 0.24	5.33 ± 0.22	5.28 ± 0.17	5.58 ± 0.21	5.06 ± 0.09	5.32 ± 0.19	5.32 ± 0.18	5.38 ± 0.11
PLT (K/µL)	592-2972	766.25 ± 126.74	789.75 ± 143.19	1070 ± 93.82	1020 ± 140.09	611.6 ± 196.51	536.2 ± 304.42	762.2 ± 327.44	502.2 ± 343.7
WBC (K/µL)	1.8-10.7	9.39 ± 1.87	6.36 ± 2.58	3.74 ± 0.61	2.94 ± 0.46	9.49 ± 2.03	12.12 ± 3.97	8.99 ± 3.91	2.94 ± 0.46
NE (K/µL)	0.1-2.4	2.05 ± 0.89	1.1 ± 0.64	1.02 ± 0.25	0.8 ± 0.08	1.75 ± 0.73	2.14 ± 0.94	2.02 ± 1.02	0.8 ± 0.08
LY (K/µL)	0.9-9.3	6.3 ± 1.23	4.54 ± 1.81	2.39 ± 0.33	1.66 ± 0.65	6.41 ± 1.25	8.29 ± 2.47	5.58 ± 2.35	1.66 ± 0.65
MO (K/µL)	0-0.4	0.67 ± 0.24	0.52 ± 0.16	0.34 ± 0.05	0.25 ± 0.05	0.67 ± 0.15	0.91 ± 0.37	0.7 ± 0.32	0.25 ± 0.05
EO (K/µL)	0-0.2	0.29 ± 0.22	0.18 ± 0.09	0.11 ± 0.05	0.19 ± 0.29	0.54 ± 0.22	0.62 ± 0.28	0.52 ± 0.29	0.19 ± 0.29
BA (K/µL)	0-0.2	0.08 ± 0.05	0.03 ± 0.01	0.03 ± 0.01	0.05 ± 0.06	0.11 ± 0.07	0.15 ± 0.1	0.16 ± 0.09	0.05 ± 0.06

All values are presented as mean ± SD (n=4-5) with corresponding normal reference ranges for mice.

References:

1. Kale VP, Hengst JA, Desai DH, et al. A novel selective multikinase inhibitor of ROCK and MRCK effectively blocks cancer cell migration and invasion. Cancer Lett. 2014;354(2):299-310.
2. Hagen JT, Montgomery MM, Aruleba RT, et al. Acute myeloid leukemia mitochondria hydrolyze ATP to support oxidative metabolism and resist chemotherapy. Sci Adv. 2025;11(15):eadu5511.
3. Ung J, Tan SF, Shaw JJP, et al. Acid ceramidase inhibition enhances BCL-2 targeting in venetoclax-resistant acute myeloid leukemia. Blood Neoplasia. 2026; 100196. doi: https://doi.org/10.1016/j.bneo.2026.100196. [Epub ahead of print]
4. Pearson JM, Tan S-F, Sharma A, et al. Ceramide Analogue SACLAC Modulates Sphingolipid Levels and MCL-1 Splicing to Induce Apoptosis in Acute Myeloid Leukemia. Molecular Cancer Research. 2020;18(3):352-363.
5. Annageldiyev C, Gowda K, Patel T, et al. The novel Isatin analog KS99 targets stemness markers in acute myeloid leukemia. Haematologica. 2020;105(3):687-696.
6. Golla U, Ehudin MA, Annageldiyev C, et al. DJ4 Targets the Rho-Associated Protein Kinase Pathway and Attenuates Disease Progression in Preclinical Murine Models of Acute Myeloid Leukemia. Cancers (Basel). 2021;13(19):4889.
7. Annageldiyev C, Tan SF, Thakur S, et al. The PI3K/AKT Pathway Inhibitor ISC-4 Induces Apoptosis and Inhibits Growth of Leukemia in Preclinical Models of Acute Myeloid Leukemia. Front Oncol. 2020;10:393.
8. Ianevski A, Giri AK, Aittokallio T. SynergyFinder 2.0: visual analytics of multi-drug combination synergies. Nucleic Acids Res. 2020;48(W1):W488-W493.
9. Bate-Eya LT, den Hartog IJ, van der Ploeg I, et al. High efficacy of the BCL-2 inhibitor ABT199 (venetoclax) in BCL-2 high-expressing neuroblastoma cell lines and xenografts and rational for combination with MCL-1 inhibition. Oncotarget. 2016;7(19):27946-27958.
10. Pan T, Wang S, Feng H, et al. Preclinical evaluation of the ROCK1 inhibitor, GSK269962A, in acute myeloid leukemia. Front Pharmacol. 2022;13:1064470.
11. Souers AJ, Leverson JD, Boghaert ER, et al. ABT-199, a potent and selective BCL-2 inhibitor, achieves antitumor activity while sparing platelets. Nat Med. 2013;19(2):202-208.
12. Leverson JD, Phillips DC, Mitten MJ, et al. Exploiting selective BCL-2 family inhibitors to dissect cell survival dependencies and define improved strategies for cancer therapy. Sci Transl Med. 2015;7(279):279ra40.
13. Stavenger RA, Cui H, Dowdell SE, et al. Discovery of aminofurazan-azabenzimidazoles as inhibitors of Rho-kinase with high kinase selectivity and antihypertensive activity. J Med Chem. 2007;50(1):2-5.
14. Safont MM, Leitch C, Popa M, et al. Protocol for the development of a bioluminescent AML-PDX mouse model for the evaluation of CAR T cell therapy. STAR Protoc. 2024;5(4):103522.
15. Annageldiyev C, Golla U, Patel S, et al. A defined culture model for ex vivo expansion of primary AML cells preserves leukemic stem cells and clonal architecture for functional and therapeutic studies. Blood. 2025;146(Supplement 1):3488-3488.
16. Paudel BB, Tan SF, Fox TE, et al. Acute myeloid leukemia stratifies as 2 clinically relevant sphingolipidomic subtypes. Blood Adv. 2024;8(5):1137-1142.
17. Chen X, Glytsou C, Zhou H, et al. Targeting Mitochondrial Structure Sensitizes Acute Myeloid Leukemia to Venetoclax Treatment. Cancer Discov. 2019;9(7):890-909.